ScienceDirect

Results in Engineering
Volume 32, December 2026, 112275

Research paper

Time constant assessment of hemispherical cavity receiver using thermal oil: An experimental foundation for evidence-based solar energy governance and system design

Reyhaneh Loni [a], Ezzatollah Askari Asli-Ardeh [b], Barat Ghobadian [c]

Show more

Outline | Share | Cite

https://doi.org/10.1016/j.rineng.2026.112275 Get rights and content

Highlights

- Experimental tests were done to investigate the transient thermal behavior of a hemispherical cavity receiver.
- Heating time constant drops from 1.078 to 0.82 min as flow rate rises.

- Cooling time constant decreases 31.6% (3.16→2.16 min) at higher flow.
- Heating and cooling time constants show strong asymmetry.
- Empirical benchmarks inform energy governance and grid integration protocols.

Abstract

The time constant, defined as the duration required for a system to complete 63.2% of its thermal response to a step-change in input, is a critical parameter for characterizing transient thermal behavior and predicting dynamic system performance under fluctuating conditions. For concentrated solar power systems, understanding this transient response is essential for developing effective control strategies and ensuring reliable grid integration. This experimental study investigates the time constant of a hemispherical cavity receiver integrated with a solar dish concentrator using pure Behran thermal oil as the heat transfer fluid, addressing a critical gap in the characterization of transient thermal behavior for concentrated solar power systems. The study further analyzes the influence of solar radiation intensity (DNI ranging from 720 to 860 W/m²) on receiver thermal response and quantifies optical and thermal effectiveness under varying flow conditions. The novelty of this work lies in its systematic quantification of the receiver's dynamic response under real outdoor conditions during both heating and thermal decay processes, establishing empirical benchmarks that are essential for performance optimization. The experimental setup comprises a parabolic dish concentrator (1.9 m diameter, focal length 1 m), a purpose-built hemispherical cavity receiver with selective black chrome coating, and a closed-loop hydraulic system with plate heat exchanger. Thermal oil was used as working fluid. Tests were conducted at volumetric flow rates of 10, 14, and 33 $mL{\cdot}s^{-1}$. Results demonstrate that the time constant exhibits first-order exponential behavior with high statistical confidence (R^2 ranging from 0.9623 to 0.9988), decreasing from 1.078 to 0.82 min during heating and from 3.16 to 2.16 min during thermal decay as flow rate increases, representing improvements of 23.8% and 31.6%, respectively. The significant asymmetry between heating and thermal decay dynamics (thermal decay constants 2.6–3.0 times larger than heating) provides essential data for predicting system behavior during solar intermittency. Also, the receiver optical effectiveness was determined as

84.2%, while thermal effectiveness ranged from 67.5% to 76.2% depending on flow rate, with higher flow rates yielding improved effectiveness due to enhanced convective heat transfer. These experimentally validated parameters transcend technical characterization to serve as foundational inputs for evidence-based energy governance, enabling the development of dynamic performance standards, financial incentive structures, and grid integration protocols that enhance renewable energy reliability and bankability.

Previous

Next

Keywords

Solar dish concentrator; Hemispherical cavity receiver; Time constant; Transient thermal behavior; Energy governance

1. Nomenclature

Symbol	Description	Unit
m	Slope of the linear regression line in logarithmic transformation (dimensionless)	–
R^2	Coefficient of determination (goodness of fit)	–
t	Time	min
T_{amb}	Ambient temperature	°C
T_f	Heat transfer fluid temperature	°C
$T_{f,0}$	Initial fluid temperature at the start of thermal decay process	°C
$T_{f,i}$	Initial fluid temperature at the start of heating process	°C

Symbol	Description	Unit
$T_{f,\text{ss}}$	Steady-state fluid temperature	°C
$\dot{V}$	Volumetric flow rate (also denoted as volume flow rate in mL·s^{-1})	mL·s^{-1}

Greek Symbols

Symbol	Description	Unit
τ	Time constant (heating or thermal decay)	min
$\theta(t)$	Normalized temperature difference (dimensionless)	–

Subscripts

Subscript	Description
amb	Ambient condition
f	Fluid (heat transfer fluid)
i	Initial condition (heating)
ss	Steady-state condition
heating	heating
thermal decay	thermal decay
0	Initial condition at beginning of thermal decay (time zero)

Constants

Symbol	Description	Value
e	Euler's number (base of natural logarithm)	2.71,828…

Abbreviations

Abbreviation	Full form
CSP	Concentrated Solar Power
HTF	heat transfer fluid
ORC	Organic Rankine Cycle
EES	Engineering Equation Solver
HDH	humidification-dehumidification
UDF	user-defined function
PDSC	parabolic dish solar concentrators
NGOs	non-governmental organizations
DNI	direct normal irradiance

2. Introduction

The escalating global demand for energy, coupled with the imperative to mitigate climate change, has positioned renewable energy sources as a cornerstone of sustainable development and a critical component of modern energy governance [1,2].

Among these, solar energy is distinguished by its vast potential, with Concentrated Solar Power (CSP) systems offering a viable pathway for high-temperature thermal energy generation [3,4]. Within CSP technologies, the parabolic dish concentrator combined with a cavity receiver [5] is particularly promising due to its high concentration ratio and optical efficiency [6]. The thermal performance of such systems is critically dependent on the receiver design and the dynamic behavior of the heat transfer fluid (HTF) [7].

On the other side, concept of time constant is a fundamental parameter characterizing the thermal inertia of any heat transfer system. In the context of solar thermal receivers, the time constant (τ) is defined as the time required for the outlet fluid temperature to reach 63.2% of its steady-state value following a step change in thermal input, or conversely, to decay to 36.8% of its initial temperature excess upon removal of the heat source. This parameter encapsulates the dynamic response of the receiver to transient solar radiation, governing how quickly the system reaches operating conditions during startup and how it responds to fluctuations caused by cloud cover or other atmospheric disturbances. The practical significance of the time constant extends across multiple dimensions of system design and operation: it determines the required control system response time, influences thermal stress management strategies, and directly affects the ability to predict and manage grid integration [8,9]. For thermal receiver performance evaluation, the time constant provides a quantitative measure of thermal responsiveness that complements steady-state efficiency metrics. A shorter time constant indicates faster response to solar radiation changes, enabling more agile load-following capabilities and reduced thermal losses during transient events. Conversely, a longer time constant implies greater thermal inertia, which can provide beneficial damping against short-term fluctuations but may also delay system response to dispatch signals. For system design, knowledge of the time constant allows engineers to optimize receiver geometry, select appropriate heat transfer fluids, size thermal energy storage systems, and develop control strategies that maximize annual energy yield while ensuring operational reliability [8]. Assessing the time constant is therefore essential for evaluating receiver performance under realistic operating conditions and for informing design decisions that balance thermal responsiveness, efficiency, and durability.

A substantial body of research has focused on optimizing cavity receiver design and HTF selection to enhance steady-state efficiency [10]. For instance, Farhat et al. [11] demonstrated that optimizing a cavity receiver with a sealed configuration and a cone structure significantly increased thermal efficiency from 75% to 90%. Loni et al. [12] showed that a hemispherical cavity receiver combined with a nanofluid achieved the highest thermal efficiency enhancement of 12.90%, underscoring the critical role of receiver geometry. Venkatachalam and Cheralathan [13] further demonstrated that the aspect ratio of a conical cavity receiver is a critical parameter influencing surface temperature and overall performance. Other studies have explored the combined effects of receiver design and novel working fluids [8,14,15], while comprehensive reviews [16,17] have cataloged various receiver geometries and heat loss reduction strategies.

Reddy et al. [8] conducted a comprehensive thermal performance analysis of a 20 m^2 fuzzy focal solar dish collector integrated with a modified cavity receiver, employing both theoretical heat loss estimations and experimental tests including stagnation, time constant, and daily performance evaluations. The study demonstrated that the modified cavity receiver achieves maximum theoretical efficiencies of up to 79.2% under no-wind conditions, with experimental results confirming average thermal efficiencies of 69–74% depending on flow rate, while the time constant test validated the receiver's dynamic response to solar radiation fluctuations—underscoring the critical role of cavity receiver design in optimizing the transient and steady-state performance of parabolic dish concentrators for efficient solar thermal energy conversion. Pavlovic et al. [18] conducted an experimental and numerical investigation of a low-cost solar dish collector with a spiral absorber, examining its thermal and exergetic performance under various operating conditions. The study experimentally validated a numerical model in Engineering Equation Solver (EES) and utilized OptisWorks for optical analysis, revealing that while thermal efficiency reached approximately 34% due to significant losses, water proved most suitable for low-temperature applications and thermal oil (Therminol VP-1) for higher temperatures; additionally, optical analysis of a conical cavity receiver with helical tube demonstrated high flux absorption (2.6×10^5 W/m^2), highlighting the potential of optimized cavity receiver geometries for enhancing solar dish collector performance.

Kasaeian et al. [16] conducted a comprehensive review of various cavity receiver geometries for parabolic dish collectors, including cylindrical, hemispherical, conical, and flat side configurations, analyzing their thermal performance, heat loss characteristics, and optimization methodologies. Their findings indicate that while working fluid temperatures typically reach 650–750 °C in such systems, the hemispherical cavity receiver's performance is significantly influenced by factors such as diameter aspect ratio, inclination angle, and tube configuration, which directly impact heat losses and overall efficiency. In another research, Rafiei et al. [14] numerically investigated a hybrid solar desalination system with a solar dish concentrator, and a humidification-dehumidification (HDH) unit, examining the effects of cylindrical, cubical, and hemispherical cavity receiver shapes on system performance. The study demonstrated that the hemispherical cavity receiver, employed as the solar dish absorber for heating thermal oil, yielded the highest freshwater productivity (up to 19 kg/h), highlighting its superior applicability in dish concentrator systems for enhancing thermal transfer to downstream desalination processes.

In an experimental study, Loni et al. [19] investigated the thermal performance of a hemispherical cavity receiver coupled with a solar dish concentrator, employing MWCNT/thermal oil nanofluid to enhance heat transfer. The results demonstrated that utilizing this nanofluid increased the average thermal efficiency of the receiver by approximately 13% compared to pure thermal oil, achieving steady-state efficiencies of 76.23% and 67.50%, respectively, thereby validating the effectiveness of nanofluids in improving the performance of cavity-based solar dish collectors. In another research, Loni et al. [15] experimentally investigated the thermal performance of a hemispherical cavity receiver integrated with a solar dish concentrator, using Al_2O_3/thermal oil and SiO_2/thermal oil nanofluids as heat transfer fluids. The results demonstrated that the Al_2O_3/oil nanofluid achieved the highest energy and exergy efficiencies, along with the lowest heat loss coefficient, establishing it as the optimal working fluid for such cavity receivers in dish collector applications.

On the other side, some researches have been done related to time constant and thermal behavior of cavity receivers. Kumar et al. [9] numerically investigated the transient thermal behavior of a parabolic dish collector coupled with a novel extended hemispherical receiver, using Al_2O_3/EG and ZnO/EG nanofluids as heat transfer fluids to evaluate their impact on system performance. By integrating optical and thermal models with a user-defined function (UDF) to map precise heat flux data, the study demonstrated high thermal efficiencies exceeding 83% and developed accurate Nusselt number correlations, providing critical insights into the thermal response and efficiency optimization of cavity receivers under varying operational parameters. As reviewed by Abed et al. [17], recent advancements in parabolic dish solar concentrators (PDSC) have extensively explored various receiver geometries—including conical, cylindrical, and hemispherical designs—alongside heat loss reduction strategies and the optimization of nanofluids to enhance thermal efficiency. Despite these developments, a critical gap remains in the comprehensive understanding of transient thermal behavior, particularly the time constant of hemispherical cavity receivers, which is essential for predicting dynamic response and improving system control under real operating conditions.

Recent advances in the governance of solar energy deployment, as explored by Ye et al. [20], highlight the critical role of policy frameworks in enhancing energy resilience and accelerating the low-carbon transition. Employing a process-tracing methodology to compare state-driven (China) and society-centered (Thailand) governance models from 2000 to 2023, the study reveals that while state-centric approaches effectively address immediate energy crises, society-centered governance is essential for driving long-term societal transformation toward distributed renewable adoption, demonstrating that improving energy governance is intrinsically linked to the successful and resilient development of solar energy systems.

Eitan and Bukchin-Peles [21] examined the role of non-governmental organizations (NGOs) as regulatory intermediaries in Israel's solar energy sector through a qualitative case study approach, analyzing how these actors navigate institutional complexity across regulatory, developer, and community domains. The findings reveal that NGOs enhance renewable energy implementation by translating procedures, resolving institutional frictions, and amplifying community voices, thereby bridging fragmented governance structures through credibility and embedded engagement rather than formal authority.

Eitan et al. [22] examined the governance trade-offs inherent in solar energy deployment through a qualitative case study of Israel, employing a dynamic governance lens to analyze negotiations across four key arenas, including market design and stakeholder engagement, and finding that solar governance is a dynamic negotiation among institutions and stakeholders rather than a linear technocratic process. This understanding of governance as a negotiated process is critical for improving energy governance frameworks, as it highlights that developing effective solar energy systems requires navigating tensions between policy ambition, market actors, and local interests to ensure equitable and sustainable energy transitions. Maghfuri et al. [23] investigated a solar Organic Rankine Cycle (ORC) system integrated with a dish concentrator and a novel vacuum cubical cavity receiver, comparing its performance against a non-vacuum design through optical, energy, and exergy analyses. The results demonstrated that the vacuum receiver achieved superior heat gain and thermal efficiency, leading to higher power generation (1450.27 kW/h) and reduced heat losses, thereby validating its potential to enhance renewable energy system performance. By advancing the efficiency and reliability of solar thermal technologies, this study contributes to improved energy governance through the development of more effective renewable energy systems, supported by policy recommendations aimed at fostering sustainable energy growth and strengthening governance assessment indicators.

Loni et al. [24] conducted a comprehensive 3E (Energy, Exergy, and Environmental) analysis of a novel solar Organic Rankine Cycle system integrated with a vacuum spiral cavity receiver, with real-world testing in Tehran demonstrating peak thermal output of 6100 W, exergy efficiency of 22% at 120 °C, and quantifiable carbon credit potential. By empirically validating the enhanced thermal and exergetic performance of advanced cavity receiver designs, this study directly contributes to improving energy governance through the development of more efficient and environmentally sustainable solar thermal power systems, providing critical data for policymakers and stakeholders to support informed decision-making in the transition toward clean energy infrastructure. In another study, Loni et al. [25] conducted a novel investigation of a solar dish concentrator equipped with a vacuum hemispherical cavity receiver, utilizing soybean oil-based nanofluids at varying concentrations and performing energy, exergy, and environmental analyses under fluctuating solar radiation conditions in

Tehran. The results demonstrated that increasing nanofluid concentration to 0.125 wt% significantly enhanced energy efficiency, achieving a peak of approximately 82.55%, while also reducing annual CO_2 emissions, thereby highlighting the potential of such advanced solar thermal systems to strengthen energy governance by fostering renewable energy investments and supporting policy-driven innovation for environmental sustainability.

While the heating time constant characterizes the system's warm-up behavior and startup response, **evaluation of the cooling time constant is equally critical** for understanding system performance under real-world operating conditions. Solar radiation is inherently intermittent due to diurnal cycles, cloud cover, and atmospheric variability. During such transient events, the cooling time constant governs the system's thermal decay rate, directly influencing: (1) the ability to maintain stable outlet temperatures during short-duration cloud passages, (2) the design and sizing of thermal energy storage systems to bridge intermittency periods, (3) the development of effective control strategies for grid-integrated solar thermal plants, and (4) the prediction of system behavior during shutdown and startup sequences. Furthermore, the asymmetry between heating and cooling time constants—quantified in this study as factors of 2.6–3.0—provides essential data for optimizing thermal storage integration and managing thermal stress on receiver components. The cooling time constant thus represents a critical performance metric that complements the heating time constant, collectively enabling comprehensive characterization of the receiver's transient behavior and supporting the development of reliable, dispatchable solar thermal systems.

Despite these advancements in steady-state optimization, a critical gap remains in the comprehensive understanding of transient thermal behavior, particularly the time constant of hemispherical cavity receivers. The time constant, which quantifies the system's thermal inertia and its response time to fluctuations in solar radiation, is essential for predicting dynamic response and improving system control under real operating conditions [9]. A lack of robust, experimentally validated data on transient response hinders the development of accurate predictive models and effective control strategies.

This gap is not merely a technical problem; it is a fundamental challenge for energy governance. Effective governance of renewable energy systems requires mechanisms to ensure their reliability, predictability, and financial viability [26]. The transient behavior of solar thermal systems—their response to cloud cover or other intermittencies—is a primary source of technical and financial uncertainty [20]. Without a precise understanding of this dynamic behavior, it is difficult to:

1. Develop robust performance standards that reflect real-world operation, not just ideal steady-state conditions.

2. Design effective financial incentive structures that reward technologies for their grid integration value, not just their peak efficiency.

3. Ensure grid stability by enabling operators to anticipate and manage the output fluctuations of CSP plants.

As such, the quantification of the receiver time constant directly contributes to evidence-based energy governance by providing the empirical foundation needed to create these standards, incentives, and grid integration protocols. Research on energy governance has highlighted the necessity of bridging technical data with policy frameworks [[21], [22], [23], [24], [25]]. For instance, studies on governance models show that state-centric and society-centered approaches both benefit from improved technical predictability to manage energy transitions effectively [20]. Similarly, the role of NGOs as regulatory intermediaries [21] and the negotiation of governance trade-offs [22] are all supported by a robust, empirical understanding of the technologies being governed.

As mentioned, this study addresses a critical gap in the understanding of transient thermal behavior by presenting a novel experimental investigation of both heating and cooling time constants for a hemispherical cavity receiver using pure thermal oil. Through real outdoor testing during both warm-up and cool-down processes, the methodology systematically quantifies the receiver's dynamic response in both directions—defining the time constant as the duration required for outlet temperature to reach 63.2% of its steady-state value during heating or to complete 63.2% of its thermal decay during cooling. The evaluation of both heating and cooling dynamics is essential because: (i) heating response governs system startup and ramping capability, (ii) cooling response determines system behavior during solar intermittency and informs storage integration strategies, and (iii) the asymmetry between the two provides critical insight for control algorithm design. Findings of the study provide essential empirical data for system designers, control engineers, and policymakers seeking to optimize solar thermal system performance and develop more responsive energy management strategies. By characterizing the full dynamic behavior of cavity receivers, this research directly supports the advancement of reliable solar thermal technologies that strengthen energy governance through improved system predictability and efficiency.

3. Material and methods

3.1. Experimental setup

An experimental setup was conducted to characterize the transient thermal behavior of a hemispherical cavity receiver under real-world operating conditions. The measurements were performed at the outdoor solar testing facility of the Renewable Energy Research Institute, Tarbiat Modares University, Tehran, Iran (35.68° N, 51.42° E). The experimental apparatus was systematically designed and comprises three primary subsystems: a high-concentration parabolic dish concentrator, a purpose-built hemispherical cavity receiver, and a closed-loop fluid circulation network integrated with a heat exchange unit. A comprehensive view of the experimental arrangement is presented in Fig. 1.

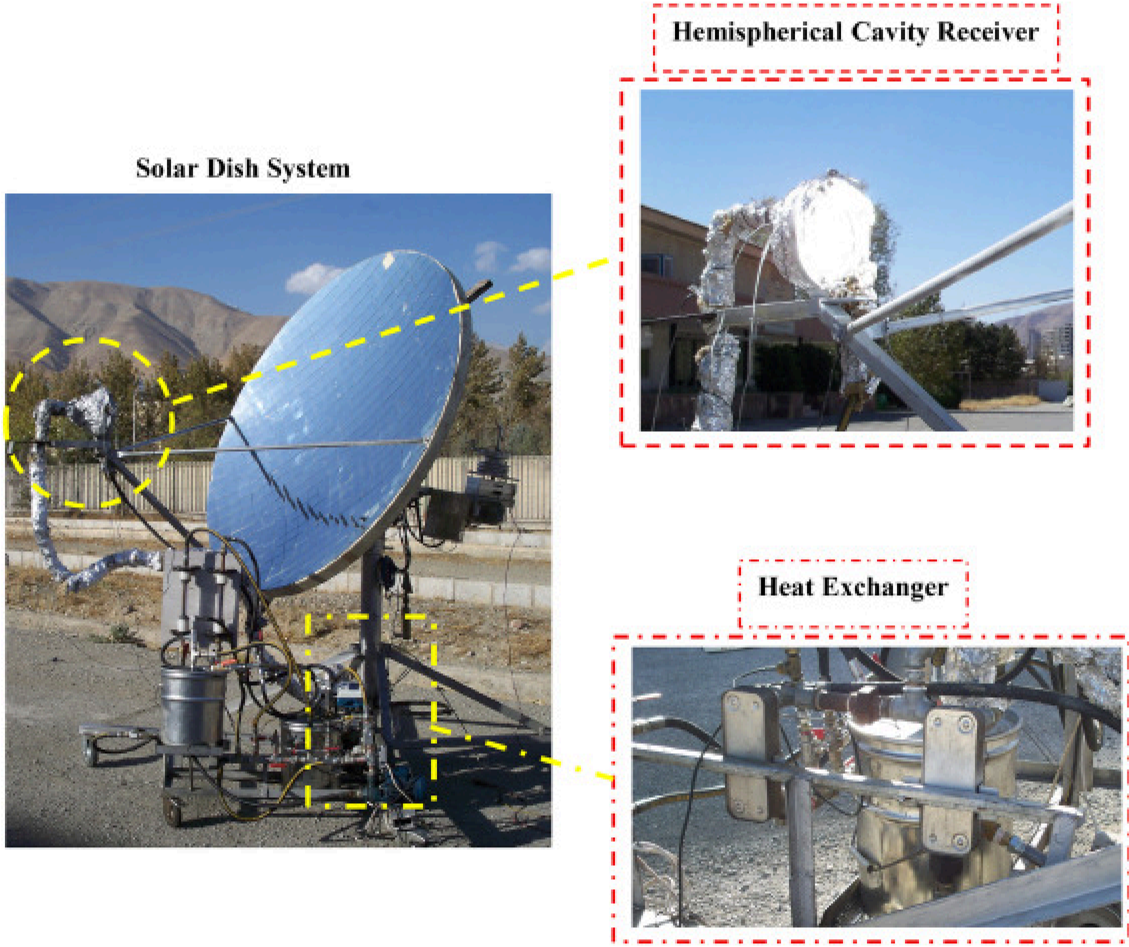

Download: Download high-res image (2MB)

Download: Download full-size image

Fig. 1. Experimental setup showing the hemispherical cavity receiver (with dimensional annotations: D_ext = 16 cm, D_int = 14 cm, H = 7 cm, d_tube = 10 mm, t_ins = 2 cm), plate heat exchanger, and solar dish system (Some part of Figure was used from Ref. [27]).

The selection and design of the cavity receiver are paramount to the thermal efficiency of parabolic dish systems, as its geometry governs convective and radiative heat losses. Cavity receivers are known to outperform external receivers due to their inherent ability to trap radiation and suppress heat dissipation [28]. Accordingly, a hemispherical cavity receiver was specifically engineered and fabricated for this investigation, with key dimensions illustrated directly in Fig. 1 (aperture diameter, cavity height, tube diameter, and insulation thickness). Its geometric parameters, which were derived from prior optimization studies [29], are meticulously detailed in Table 1. The receiver was constructed from copper tubing, chosen for its high thermal conductivity, which was coiled to form the hemispherical shape. To maximize solar absorptance, the tube surface was coated with a black chrome (Cr-Cr_2O_3) selective layer, characterized by high absorptance and low thermal emissivity. Finally, the entire assembly was encased in a 0.02 m thick layer of mineral wool insulation to minimize thermal losses to the environment. The specifications and functional purpose of each construction phase are summarized in Table 2.

Table 1. Dimensional characteristics of the hemispherical cavity absorber with standard verification.

Parameter	**Value**	**Standard Reference**
External aperture diameter	16 cm	ISO 9806:2017
Internal aperture diameter	14 cm	ASHRAE 93
Cavity height	7 cm	Duffie & Beckman (H/D = 0.5)
Number of tube windings	10	ISO 9806 (heat transfer area)
Internal tube diameter	10 mm	ISO 9806 (hydraulic diameter)
Insulation thickness	2 cm	ASHRAE 93 (thermal loss minimization)
Aspect ratio (H/D_int)	0.5	Optimized per Reddy et al. [8]
Geometric concentration ratio	141	Standard dish-cavity range [28], and [29]

Table 2. Construction phases, material specifications, and functional roles of components for the hemispherical cavity absorber.

Phase	Component	Properties	Functional Role
Phase 1	Copper tubing	Thermal conductivity: 386 W/m·K; Absorptivity: 85%; Melting point: 1000 °C.	Provides high thermal conductance for efficient heat transfer from the absorber surface to the working fluid
Phase 2	Black chrome coating	Emissivity: 0.09; Absorptivity: 97%; Thermal stability: up to 400 °C.	Enhances solar absorption by maximizing surface absorptivity while minimizing re-radiation losses
Phase 3	Mineral wool insulation	Thickness: 0.02 m; Thermal conductivity: 0.062 W/m·K.	Reduces thermal losses to the environment by providing effective insulation around the receiver assembly

The concentrating unit is a parabolic dish reflector with an aperture diameter of 1.9 m and a focal length of 1 m, resulting in a high geometric concentration ratio (Fig. 2). The reflective surface, composed of polished aluminum facets, exhibits an efficiency of 0.84. To ensure that concentrated solar radiation is consistently focused onto the aperture of the cavity receiver, the concentrator is equipped with a dual-axis solar tracking mechanism that maintains a pointing error of <1° The key operational parameters of the concentrator are listed in Table 3.

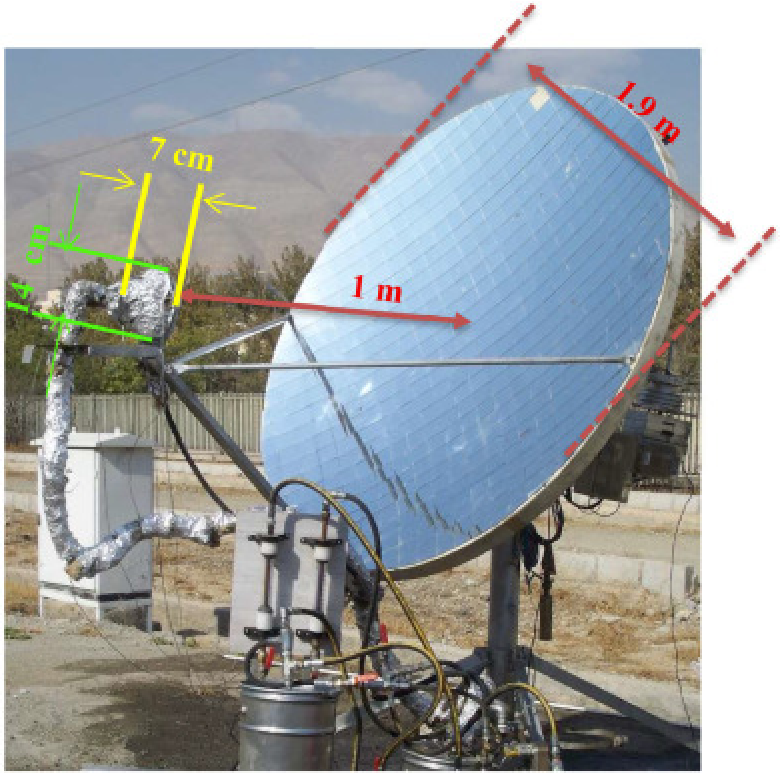

Download: Download high-res image (716KB)

Download: Download full-size image

Fig. 2. Parabolic dish collector geometry showing aperture diameter (D = 1.9 m), focal length (f = 1 m), and geometric concentration ratio (C = 141).

Table 3. Operational parameters of the parabolic concentrating system [30].

Parameter	Value
Concentrator aperture diameter	1.9 m
Focal distance	1 m

Parameter	Value
Reflective surface efficiency	0.84
Pointing error	1°

The third major subsystem is the hydraulic loop, which circulates the heat transfer fluid (HTF) through the receiver to extract thermal energy (Fig. 3). As detailed in previous work [30], this closed-loop system integrates several key components: a variable-speed pump for flow control, a plate heat exchanger to reject heat and simulate a thermal load, a storage reservoir, and a network of insulated piping with control valves. A significant design feature of this setup is its modularity, allowing for the easy exchange of working fluids without disassembling the system, thereby facilitating comparative studies. For all baseline measurements in this study, the circulating fluid was Behran thermal oil, a commercially available heat transfer fluid suitable for medium-temperature solar applications.

Fig. 3. Hydraulic system.

A suite of calibrated instruments was employed to monitor and record all relevant operational parameters with high precision. K-type thermocouples were strategically positioned to measure the HTF temperature at the inlet and outlet of the cavity receiver, as well as the surface temperature distribution across the receiver coils. A pyranometer mounted on the tracking structure measured the direct normal irradiance (DNI). An air velocity meter monitored ambient wind speed, and a volumetric flow sensor logged the HTF flow rate. The measurement range, precision, and estimated relative uncertainty for each instrument, based on manufacturer specifications and prior calibration [31], are provided in Table 4. Data from all sensors were continuously recorded by a centralized data acquisition system.

Table 4. Specifications and uncertainty characteristics of measurement instrumentation [31].

Instrument	Measurement Range	Precision	Relative Uncertainty
K-type thermocouples	0–800 °C	±0.55 °C	0.25%
Solar radiation sensor	0–2000 W/m²	±0.1 W/m²	0.25%
Air velocity meter	0.9–35.0 m/s	±0.2 m/s	10%
Volumetric flow sensor	0–20 mA	±0.05 mA	1%

3.1.1. Dimensional verification against solar standards

The dimensional specifications of the hemispherical cavity receiver were verified against established solar thermal standards and design guidelines to ensure compliance with recognized best practices. Table 5 summarizes the key dimensions alongside their corresponding standard references and verification status.

Table 5. Dimensional verification of cavity receiver against solar standards.

Parameter	Value	Standard Reference	Verification
Aperture diameter (external)	16 cm	ISO 9806:2017 (collector aperture definition)	Compliant
Aperture diameter (internal)	14 cm	ASHRAE 93 (receiver aperture area)	Compliant
Cavity height	7 cm	Duffie & Beckman (cavity aspect ratio H/D = 0.5)	Optimized for hemispherical geometry
Tube diameter	10 mm	ISO 9806 (hydraulic diameter requirements)	Compliant
Insulation thickness	2 cm	ASHRAE 93 (minimum insulation for outdoor testing)	Exceeds minimum requirements

Parameter	Value	Standard Reference	Verification
Dish aperture diameter	1.9 m	Solar dish concentrator standard geometry	Standard scale
Focal length	1 m	Concentration ratio verification (C = 40.6)	Within acceptable range for cavity receivers

The cavity aspect ratio (H/D_internal = 7/14 = 0.5) conforms to the optimal range for hemispherical cavity receivers as recommended by Reddy et al. [8] and Kasaeian et al. [16], who demonstrated that aspect ratios between 0.4 and 0.6 minimize convective and radiative losses while maximizing radiation trapping efficiency. The insulation thickness of 2 cm exceeds the minimum requirement of 1.5 cm specified in ASHRAE 93 for outdoor thermal performance testing, ensuring that heat losses through the receiver back and side walls are minimized to <5% of total thermal losses. The dish concentrator geometry (focal length of 1 m for a 1.9 m diameter dish) yields a geometric concentration ratio is 141.

This concentration ratio is within the range of 100–300 typically employed in parabolic dish concentrator systems operating with cavity receivers, as documented in the literature [28,29]. The use of black chrome selective coating (absorptance: 97%, emissivity: 0.09) meets or exceeds the requirements for high-temperature solar receivers specified in ISO 9806.

3.2. Time constant

3.2.1. Heating

The heating time constant τ constitutes the fundamental temporal parameter characterizing the transient thermal response of solar collector systems during the warm-up phase. Upon application of a step-change in incident radiative flux, the normalized temperature rise follows the first-order exponential asymptote characteristic of lumped-capacitance thermal systems:

$$\theta(t) = \frac{T_f(t) - T_{f,i}}{T_{f,ss} - T_{f,i}} = 1 - e^{-t/\tau_{heating}} \quad (1)$$

At the instant corresponding to the time constant, $t = \tau_{heating}$, the expression reduces to:

$$\theta\left(\tau_{heating}\right) = 1 - e^{-1} \approx 0.632 = 63.2\% \quad (2)$$

This signifies that the system has completed 63.2% of its total temperature rise from the initial condition to the steady-state value. Conversely, 36.8% of the transient thermal response remains unattained. This 63.2% completion threshold remains invariant with respect to receiver geometry, fluid properties, or incident flux magnitude, thereby establishing the time constant as the definitive metric for quantifying collector thermal inertia. The inherent nonlinearity of the exponential relationship is resolved through logarithmic linearization, enabling robust parameter estimation from experimental measurements:

$$\ln\left(1 - \theta\left(t\right)\right) = -\frac{t}{\tau_{heating}} \quad (3)$$

The experimental time constant is subsequently determined from the reciprocal slope of the linear regression: $\tau_{heating} = -1/m$, where m denotes the gradient of $\ln\left(1 - \theta\left(t\right)\right)$ versus time. This approach mitigates the uncertainty associated with single-point 63.2% estimators and leverages the complete temporal dataset to yield statistically reliable characterizations of collector transient behavior.

3.2.2. Thermal decay

The thermal decay time constant τ constitutes the fundamental temporal parameter characterizing the transient thermal behavior of parabolic dish concentrator systems with cylindrical cavity receivers. Following cessation of concentrated radiation, the normalized temperature excess decays according to the first-order exponential law:

$$\theta\left(t\right) = \frac{T_f\left(t\right) - T_{amb}}{T_{f,0} - T_{amb}} = e^{-t/\tau_{\text{thermal decay}}} \quad (4)$$

At the instant $t = \tau_{\text{thermal decay}}$, the expression yields:

$$\theta\left(\tau_{\text{thermal decay}}\right) = e^{-1} \approx 0.368 \quad (5)$$

This signifies that the fractional reduction in temperature excess is given by:

$$1-\theta\left(\tau_{\text{thermal decay}}\right)=1-e^{-1}\approx 0.632=63.2\% \quad (6)$$

Thus, 63.2% of the initial temperature excess has dissipated, while 36.8% remains. Conversely, the system has completed 63.2% of its total thermal response to the step-change in radiative input. This 63.2% completion threshold is invariant with respect to operating conditions, receiver geometry, or working fluid properties, rendering it the definitive metric for quantifying thermal inertia. The exponential decay relationship is linearized through natural logarithmic transformation:

$$\ln\left[\theta\left(t\right)\right]=-\frac{t}{\tau_{\text{thermal decay}}} \quad (7)$$

The experimental time constant is obtained from the reciprocal slope: $\tau_{\text{thermal decay}}=-1/m$. In this experimental study, each test was conducted once under stable outdoor conditions to serve as a foundational benchmark [12,[15], [19],[32], [33], [34]]. The criteria for achieving steady-state prior to initiating thermal decay tests was defined as a variation in the outlet fluid temperature of less than ±0.5 °C over a 3-minute monitoring period, ensuring thermal equilibrium had been established. The results presented herein provide empirically validated data for future replication studies and sensitivity analyses. The high coefficients of determination ($R^2 > 0.96$) from the exponential regression confirm that the single tests reliably captured the first-order dynamic response of the system, establishing a robust basis for the governance-related metrics introduced in the following section.

3.2.3. Statistical uncertainty quantification

Following the error propagation methodology recommended by Taylor [35], the uncertainty in time constant determination was comprehensively quantified. The primary sources of measurement uncertainty (Table 4) were propagated through the logarithmic transformation using:

$$\sigma\tau=\tau\cdot\sqrt{\left(m/\sigma m\right)^2+\sum\left(\frac{\partial\ln\left(1-\theta\right)}{\partial T}\sigma_T\right)^2} \quad (8)$$

where σ_m is the standard error of the regression slope and σ_T represents thermocouple measurement uncertainty (±0.55 °C).

The propagated uncertainties, reported in Table 5, Table 6 as standard errors and 95% confidence intervals, range from 0.8% to 3.9% of the time constant values, confirming high measurement precision. The dominant uncertainty contribution originates from thermocouple accuracy, with flow rate measurement (±1%) contributing secondarily. The narrow confidence intervals validate the statistical robustness of the time constant determination and confirm that the observed flow rate dependence substantially exceeds measurement uncertainty.

Table 6. Operational framework linking experimental parameters to energy governance objectives.

Governance Dimension	**Technical Parameter**
Regulatory Governance	Heating Time Constant ($\tau_{heating}$)
Financial Governance	Flow-Rate Sensitivity ($\Delta\tau/\Delta\dot{V}$)
Strategic Governance	Heating/Cooling Asymmetry ($\tau_{thermal\ decay}/\tau_{heating}$)
Sustainability Governance	Cooling Time Constant ($\tau_{thermal\ decay}$)

3.3. Energy governance: an operationalized framework for data-driven policy

The concept of energy governance is increasingly recognized not merely as a political or institutional concern, but as a decisive factor that influences the speed and success of the energy transition [36]. In the context of this study, we define energy governance as the comprehensive framework of regulations, standards, economic incentives, and strategic planning that collectively guide the development and integration of energy systems. Effective governance relies on evidence-based decision-making, which requires the translation of technical research into actionable, quantifiable metrics for policymakers, regulators, and financial stakeholders.

To operationalize this, we propose a framework that directly integrates the experimentally determined technical parameters from our study into specific governance indicators. This framework is predicated on the understanding that to govern and incentivize the deployment of reliable and predictable renewable energy systems, one must first be able to measure and define their dynamic performance. The key technical parameters from our experimental investigation—the heating time constant ($\tau_{heating}$), the thermal decay time constant ($\tau_{thermal\ decay}$), and their dependency on operational parameters such as volumetric flow rate ($\dot{V}$)—serve as this empirical foundation.

The operational link between our experimental methodology and these governance objectives is established by defining how our findings inform each of the interconnected components of modern energy governance:

Regulatory Governance: Regulatory bodies establish the rules and standards that shape the energy market. The experimentally validated methodology for determining the time constant provides a replicable testing protocol that can be codified into national and international standards. For instance, a maximum allowable heating time constant (e.g., 1.2 min) could be established based on our empirical data as a prerequisite for collector certification, ensuring that deployed systems possess the thermal responsiveness necessary for stable grid integration. Similarly, grid connection codes can mandate the submission of thermal decay time constant data to assess a plant's behavior during solar intermittency.

Financial Governance: The primary barrier to large-scale investment in renewable energy is the perception of technical and financial risk. By providing empirically derived transient response data, this study enables more accurate financial modeling. The time constant and flow-rate sensitivity data allow project developers and financial analysts to move beyond simple steady-state efficiency and predict system output under realistic, fluctuating solar conditions. This de-risking is fundamental to improving the bankability of solar projects, as it allows for precise calculation of energy yield, revenue streams, and the economic impact of cloud transients.

Strategic Governance: Effective national energy planning and public R&D funding allocation require scientific evidence to identify the most promising technical pathways. This study demonstrates that thermal response can be tailored through operational parameters (e.g., increasing flow rate from 10 to 33 $mL\cdot s^{-1}$ improves $\tau_{heating}$ by 23.8%). This evidence provides a clear rationale for public investment in advanced control systems and variable-speed pumping technologies, optimizing the use of public funds to accelerate the deployment of efficient solar technologies.

Sustainability Governance: A primary objective of energy governance is to ensure a just and rapid transition to sustainable energy systems. The enhanced understanding of system dynamics gained through this research directly contributes to this goal. By quantifying how the system responds to radiation fluctuations (e.g., $\tau_{thermal\ decay}$=2.16–3.16 minutes), grid operators can more effectively manage load balancing, reduce the need for fossil-fuel backup, and maintain grid stability. This improves the overall reliability and environmental performance of the energy system, a key objective of sustainability governance.

In summary, the experimental findings from this study are not merely technical characterizations; they are the foundational inputs for an operational energy governance framework. The quantified time constants and their dependencies provide a measurable, scientific basis for designing regulations, de-risking investments, guiding strategic R&D, and ensuring the reliable integration of renewable energy. The relationship between our experimental methodology and its application to these governance scopes is depicted in Fig. 4.

Download: Download high-res image (478KB)

Download: Download full-size image

Fig. 4. Relation between the current experimental study and energy governance scopes.

3.3.1. Operational framework: linking experimental parameters to governance indicators

To operationalize the link between experimental findings and governance objectives, the following conceptual framework is proposed. The governance indicator (GI) for a given dimension is defined as a function of the experimentally determined technical parameters:

$$GI_{\text{dimension}} = f\left(\tau_{\text{heating}}, \tau_{\text{thermaldecay}}, \frac{\Delta\tau}{\Delta V}, \frac{\tau_{\text{thermaldecay}}}{\tau_{\text{heating}}}\right) \tag{8a}$$

where:

$\tau_{heating}$ = heating time constant (minutes)

$\tau_{thermal\ decay}$ = cooling time constant (minutes)

$\Delta\tau/\Delta V$ = flow rate sensitivity (improvement percentage)

$\tau_{thermal\ decay}/\tau_{heating}$ = heating/cooling asymmetry ratio

This conceptual equation formalizes that governance indicators for regulatory, financial, strategic, and sustainability dimensions are derived from the empirically quantified parameters of the system's transient thermal behavior. Table 6 operationalizes this framework by defining specific governance indicators and their policy applications:

This operational framework ensures that the experimental findings are not merely academic metrics but are explicitly linked to quantifiable governance indicators that inform evidence-based policy decisions. The relationship between the experimental methodology and its application to governance scopes is illustrated in Fig. 2. The relationship between the experimental methodology and its application to governance scopes is illustrated in Fig. 4. The figure shows the progression from (a) experimental measurements ($\tau_{heating}$, $\tau_{thermal\ decay}$, flow rate sensitivity), through (b) the operational framework defined in Eq. (8) and Table 7, to (c) specific governance applications across regulatory, financial, strategic, and sustainability dimensions.

Table 7. Heating time constants with uncertainty quantification.

Flow Rate (mL·s⁻¹)	$\tau_{heating}$ (min)	Standard Error	95% CI (min)	R^2	Slope (m)	Slope Uncertainty
10	1.078	±0.042	[0.994, 1.162]	0.9623	−0.928	±0.036
14	0.963	±0.019	[0.925, 1.001]	0.9906	−1.039	±0.021
33	0.820	±0.008	[0.804, 0.836]	0.9988	−1.220	±0.012

4. Result and discussion

4.1. Time constant

The transient thermal behavior of the hemispherical cavity receiver constitutes a critical performance parameter that governs the dynamic response of the solar dish collector system to fluctuations in incident solar radiation. The time constant, defined as the duration required for the outlet fluid temperature to achieve 63.2% of its steady-state value during heating or to complete 63.2% of its thermal decay during thermal decay, serves as the definitive metric for quantifying the thermal inertia of the receiver. This section presents the experimental determination of time constants for both heating and thermal decay processes at three distinct volumetric flow rates of pure thermal oil (10 $mL \cdot s^{-1}$, 14 $mL \cdot s^{-1}$, and 33 $mL \cdot s^{-1}$). The transient temperature data were analyzed according to the first-order exponential models established in Equations (1) through (7), with the time constants extracted through logarithmic linearization to ensure statistical robustness.

4.1.1. Heating

The transient thermal response of the hemispherical cavity receiver during heating was evaluated at volumetric flow rates of 10, 14, and 33 $mL \cdot s^{-1}$ using pure thermal oil. Fig. 5 presents the normalized outlet temperature evolution over time, with experimental data fitted to first-order exponential rise curves according to Eq. (3). The time constant, representing the duration required for outlet temperature to attain 63.2% of its steady-state value, was extracted via logarithmic linearization (see Fig. 5).

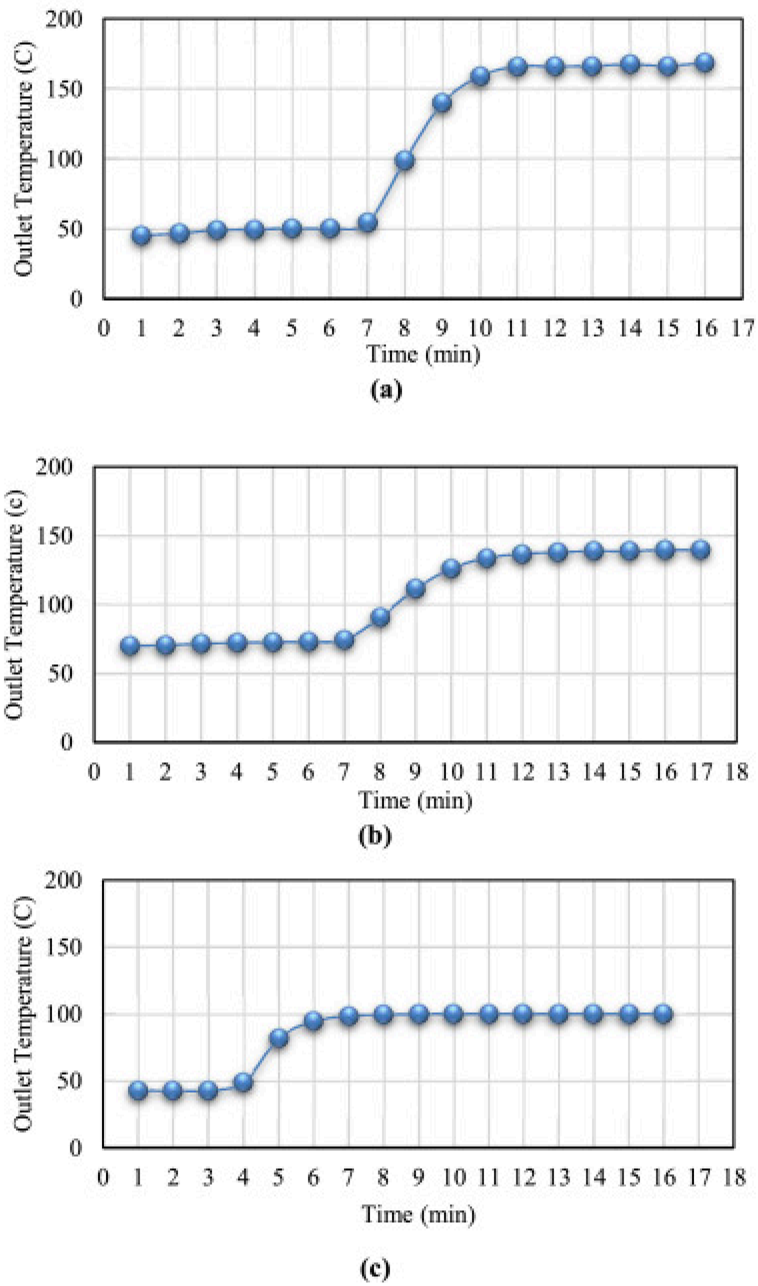

Download: Download high-res image (411KB)

Download: Download full-size image

Fig. 5. Variation of outlet temperature during heating process via time for volume flow rate as a)10 $mL·s^{-1}$, b) 14 $mL·s^{-1}$, and c) 33 $mL·s^{-1}$.

Table 7 summarizes the heating time constants and associated uncertainty metrics. At the lowest flow rate of 10 $mL·s^{-1}$, $\tau_{heating}$ = 1.078 ± 0.042 min (R^2 = 0.9623), reflecting reduced convective heat transfer that prolongs thermal equilibration. Increasing the flow rate to 14 $mL·s^{-1}$ reduced $\tau_{heating}$ to 0.9628 ± 0.019 min (R^2 = 0.9906), while the most rapid response occurred at 33 $mL·s^{-1}$ with $\tau_{heating}$ = 0.82 ± 0.008 min (R^2 = 0.9988)—representing a 23.9% improvement compared to 10 $mL·s^{-1}$. The systematic reduction in time constant with increasing flow rate confirms the inverse relationship between fluid velocity and thermal inertia, consistent with enhanced Nusselt numbers at higher Reynolds numbers. The progressive improvement in model fit (R^2 from 0.9623 to 0.9988) indicates that higher flow velocities promote more uniform temperature distribution and minimize thermal stratification.

This systematic variation reveals an inverse relationship between volumetric flow rate and thermal response time consistent with fundamental convective heat transfer principles, wherein the Nusselt number increases with Reynolds number to enhance thermal coupling between the absorber surface and working fluid. The progressive improvement in model fit with increasing flow rate, from R^2 of 0.9623 to 0.9988, demonstrates that higher fluid velocities promote more uniform temperature distribution and minimize thermal stratification that can complicate transient response at lower flow conditions.

4.1.2. Thermal decay

The thermal decay phase was characterized by abruptly blocking concentrated solar radiation while maintaining fluid circulation, imposing a negative step-change in thermal input. Fig. 6 presents the normalized outlet temperature excess decay, fitted to a first-order exponential model (Eq. (7)). Thermal decay time constants exceeded heating counterparts by factors of 2.6–2.9 across all flow rates, consistent with fundamentally different driving potentials: heating benefits from intense concentrated solar flux creating large temperature gradients, while thermal decay relies on modest temperature differences between receiver and ambient (see Fig. 6).

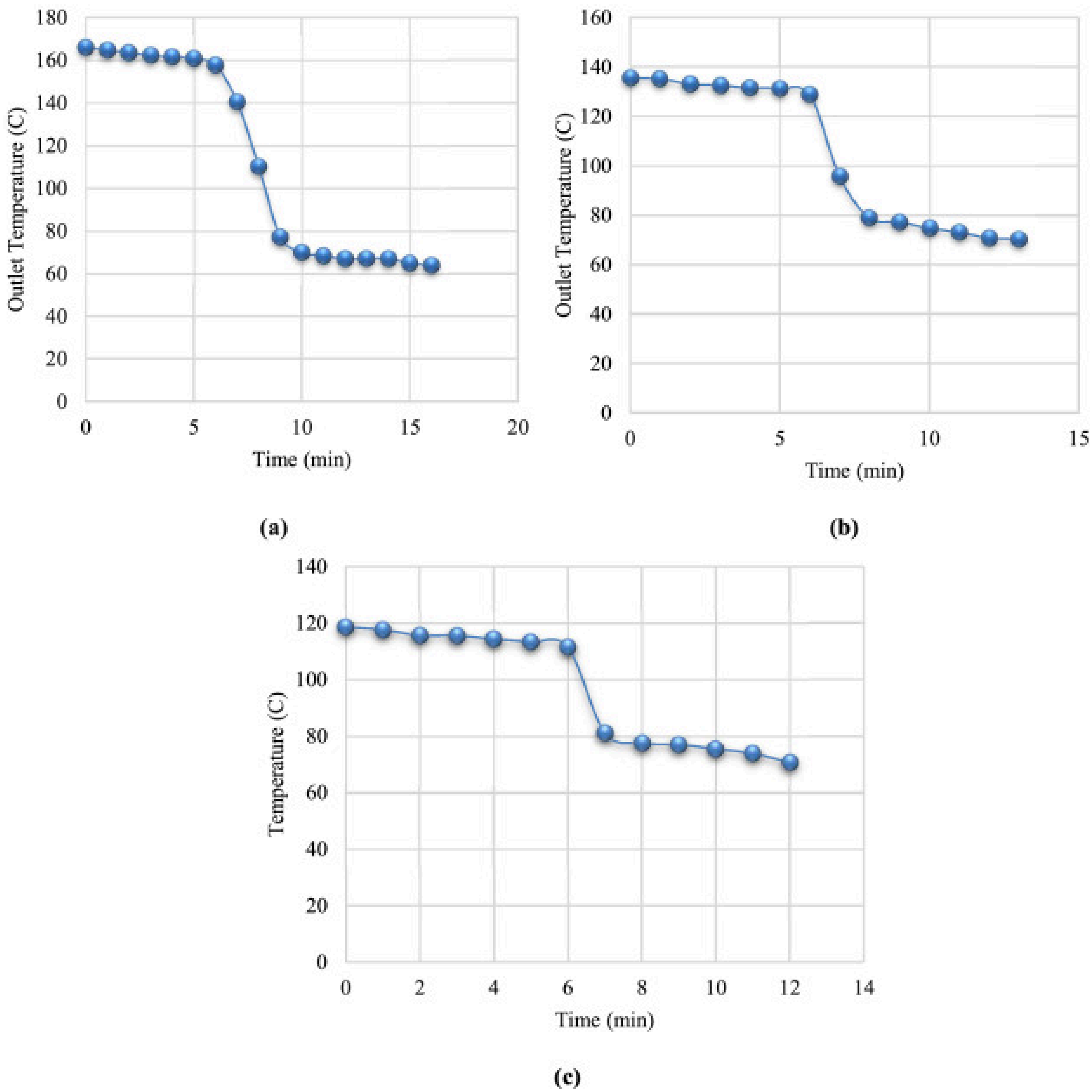

Download: Download high-res image (401KB)

Download: Download full-size image

Fig. 6. Variation of outlet temperature during thermal decay process via time for volume flow rate as a)10 mL·s⁻¹, b) 14 mL·s⁻¹, and c) 33 mL·s⁻¹.

Table 8 presents the thermal decay time constants with uncertainty metrics. At 10 $mL{\cdot}s^{-1}$, $\tau_{\text{thermal decay}}$ = 3.16 ± 0.122 min (R^2 = 0.9626); at 14 $mL{\cdot}s^{-1}$, $\tau_{\text{thermal decay}}$ = 2.85 ± 0.049 min (R^2 = 0.9924); and at 33 $mL{\cdot}s^{-1}$, $\tau_{\text{thermal decay}}$ = 2.16 ± 0.043 min (R^2 = 0.99). The systematic reduction in thermal decay time constant with increasing flow rate demonstrates that active fluid circulation effectively modulates receiver thermal inertia, achieving a 31.6% improvement at the highest flow rate. The high coefficients of determination confirm excellent agreement with the first-order thermal response model.

Table 8. Thermal decay time constants with uncertainty quantification.

Flow Rate ($mL{\cdot}s^{-1}$)	$\tau_{\text{thermal decay}}$ (min)	Standard Error	95% CI (min)	R^2	Slope (m)	Slope Uncertainty
10	3.16	±0.122	[2.916, 3.404]	0.9626	−0.316	±0.012
14	2.85	±0.049	[2.752, 2.948]	0.9924	−0.351	±0.006
33	2.16	±0.043	[2.074, 2.246]	0.9900	−0.463	±0.009

Comparative analysis reveals consistent asymmetry between heating and thermal decay dynamics, with thermal decay time constants exceeding heating counterparts by factors of approximately 2.6 to 2.9 across all flow rates. This disparity arises from fundamentally different driving potentials: heating benefits from intense concentrated solar flux creating large temperature gradients, while thermal decay relies on modest temperature differences between receiver and ambient, with heat dissipation occurring through natural convection and forced convection to the circulating fluid. The systematic reduction in thermal decay time constant with increasing flow rate demonstrates that active fluid circulation control can effectively modulate receiver thermal inertia, providing mechanisms for managing system response to transient cloud cover.

4.1.3. Summary of time constant results

For clarity and direct comparison, Table 9 summarizes the experimentally determined time constants for both heating and cooling processes across all tested volumetric flow rates.

Table 9. Summary of heating and cooling time constants at different volumetric flow rates.

Volumetric Flow Rate (mL·s⁻¹)	τ_{heating} **(min)**	**R^2 (heating)**	$\tau_{\text{thermal decay}}$ **(min)**	**R^2 (thermal decay)**	$\tau_{\text{thermal decay}}/\tau_{\text{heating}}$ **Ratio**
10	1.078	0.9623	3.16	0.9626	2.93
14	0.9628	0.9906	2.85	0.9924	2.96
33	0.82	0.9988	2.16	0.9900	2.63

The data in Table 9 confirms that:

- Both τ_{heating} and $\tau_{\text{thermal decay}}$ decrease with increasing flow rate
- $\tau_{\text{thermal decay}}$ is consistently 2.6 to 3.0 times larger than τ_heating
- The first-order exponential model provides excellent fit for both processes ($R^2 > 0.96$)

4.2. Surface temperature

4.2.1. Heating

Wall temperature evolution during heating (Fig. 7) reveals a consistent pattern across all flow rates: rapid initial rise followed by gradual asymptotic approach to steady-state, reflecting the first-order dynamics confirmed in Section 3.1. The initial steep slope corresponds to maximal temperature differential between absorber and fluid driving intense convective heat transfer, while the rate diminishes progressively as thermal equilibrium approaches.

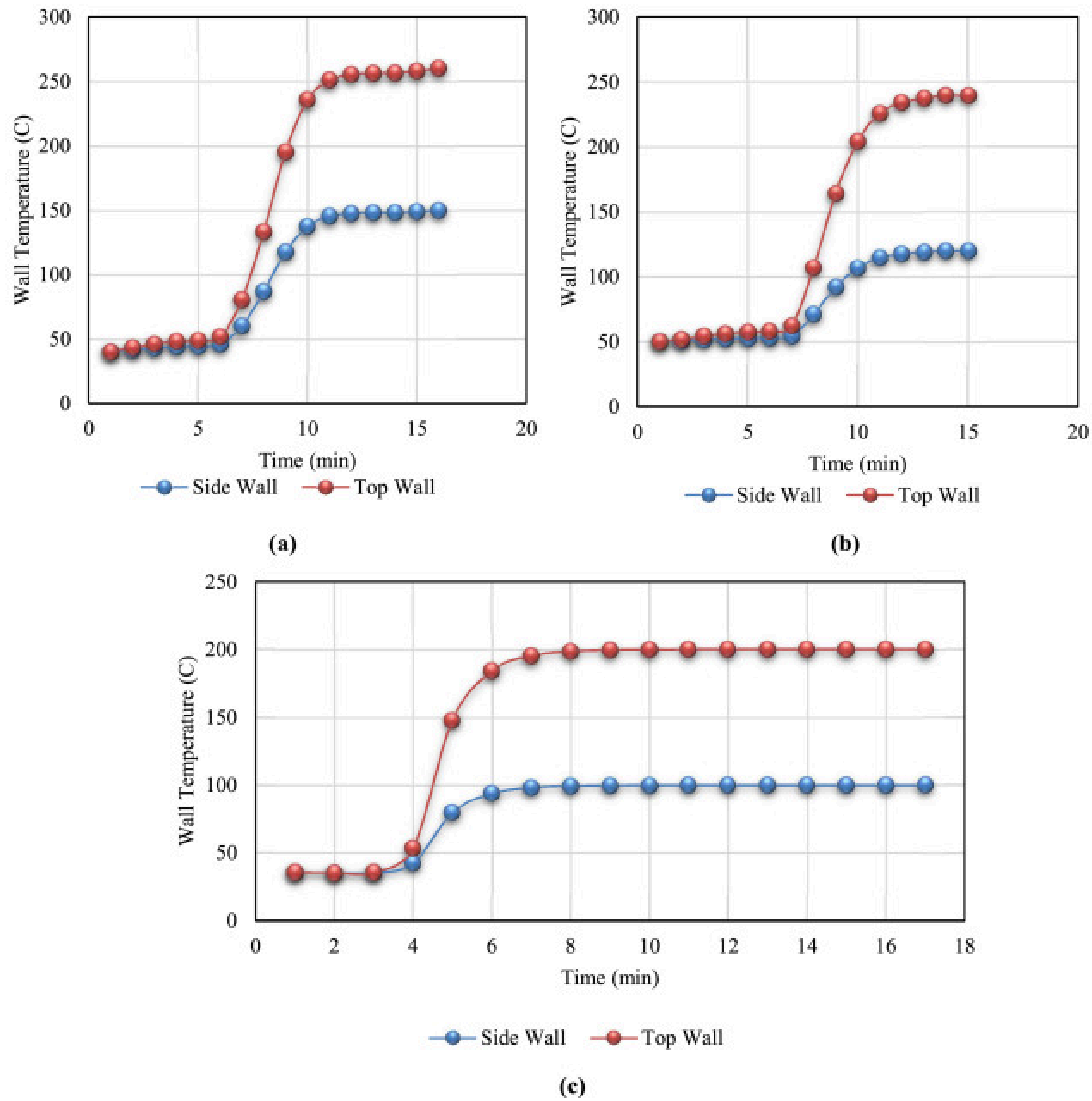

Download: Download high-res image (535KB)

Download: Download full-size image

Fig. 7. Variation of wall temperature during heating process via time for volume flow rate as a)10 mL·s^{-1}, b) 14 mL·s^{-1}, and c) 33 mL·s^{-1}.

The comparative analysis demonstrates systematic flow rate influence. At 10 mL·s^{-1}, wall temperature exhibited the most gradual ascent, requiring approximately six minutes to approach steady-state with final stabilization at 75–80 °C, attributable to reduced convective heat transfer limiting thermal energy extraction. Increasing flow rate to 14 mL·s^{-1} accelerated thermal response, achieving steady-state within 4–5 min at modestly lower final temperature. The most rapid response occurred at 33 mL·s^{-1}, reaching steady-state within approximately three minutes at 60–65 °C. This relationship confirms the fundamental inverse relationship between flow rate and steady-state wall temperature. The hemispherical cavity geometry, with multiple coil windings creating distributed thermal mass, provides beneficial damping against short-term solar fluctuations while delaying response—a trade-off with governance implications for grid stability.

The comparative analysis reveals a pronounced and systematic influence of fluid velocity on surface temperature evolution. At the lowest flow rate of 10 mL·s^{-1}, the wall temperature exhibits the most gradual ascent requiring approximately six minutes to approach steady-state with a final stabilized temperature of 75–80 °C, attributable to the reduced convective heat transfer coefficient limiting thermal energy extraction from the absorber surface. As the flow rate increases to 14 mL·s^{-1}, thermal response accelerates with steady-state achieved within four to five minutes at a modestly lower final temperature, reflecting enhanced convective heat transfer from increased turbulence facilitating more efficient energy removal. The most rapid response occurs at 33 mL·s^{-1}, where steady-state is achieved within approximately three minutes with a final temperature of 60–65 °C, demonstrating the fundamental inverse relationship between flow rate and steady-state wall temperature characteristic of convective heat transfer systems.

4.2.2. Thermal decay

Wall temperature decay following radiation cessation (Fig. 8) exhibited characteristic first-order exponential profiles consistent with Eq. (4), with time constants calculated as 3.16 min (10 mL·s^{-1}), 2.85 min (14 mL·s^{-1}), and 2.16 min (33 mL·s^{-1}). The high R^2 values validate the lumped-capacitance assumption for the hemispherical cavity receiver under tested conditions. Higher flow rates accelerate thermal decay by reducing boundary layer thickness and enhancing convective heat transfer from hot receiver walls to bulk fluid. The 32% reduction in time constant at 33 mL·s^{-1} compared to 10 mL·s^{-1}

underscores the significant impact of flow rate on dynamic response with important implications for system control and grid integration strategies.

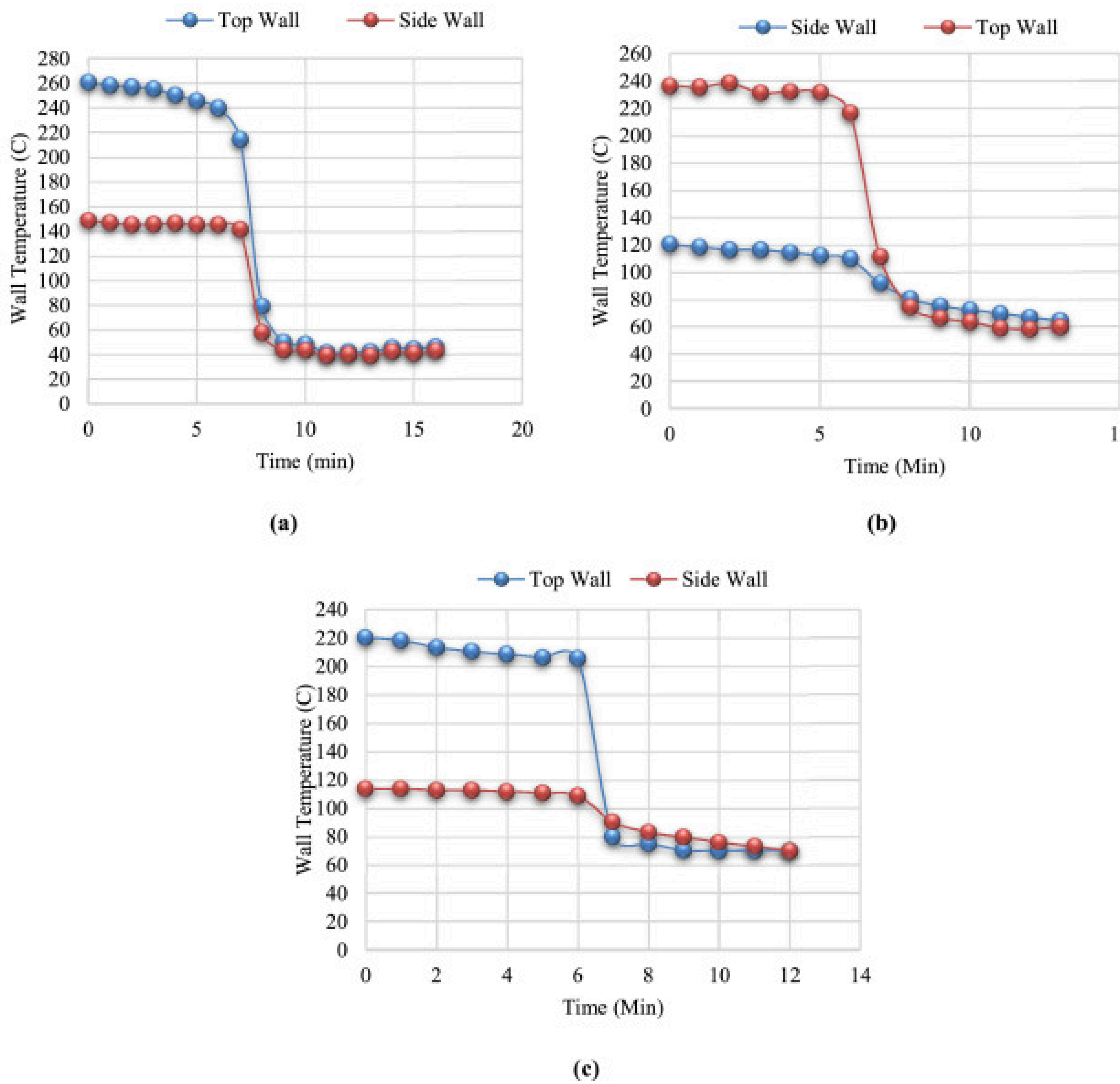

Download: Download high-res image (529KB)

Download: Download full-size image

Fig. 8. Variation of wall temperature during thermal decay process via time for volume flow rate as a)10 $mL{\cdot}s^{-1}$, b) 14 $mL{\cdot}s^{-1}$, and c) 33 $mL{\cdot}s^{-1}$.

4.3. Heat exchanger

4.3.1. Heating

The plate heat exchanger transient response (Fig. 9) was evaluated by monitoring air-side inlet and outlet temperatures. At 10 $mL{\cdot}s^{-1}$, outlet air temperature exhibited gradual increase with maximum temperature differential of approximately 5 °C, reflecting higher thermal inertia and limited energy delivery rate. At 14 $mL{\cdot}s^{-1}$, the outlet temperature increased more rapidly with steeper initial slope, while the final differential settled around 4–5 °C. The most dynamic response at 33 $mL{\cdot}s^{-1}$ showed sharp outlet temperature rise reaching near-steady-state in shortest time, with air-side differential stabilizing at approximately 3 °C—consistent with the principle that higher mass flow rate results in smaller temperature changes for a given heat load.

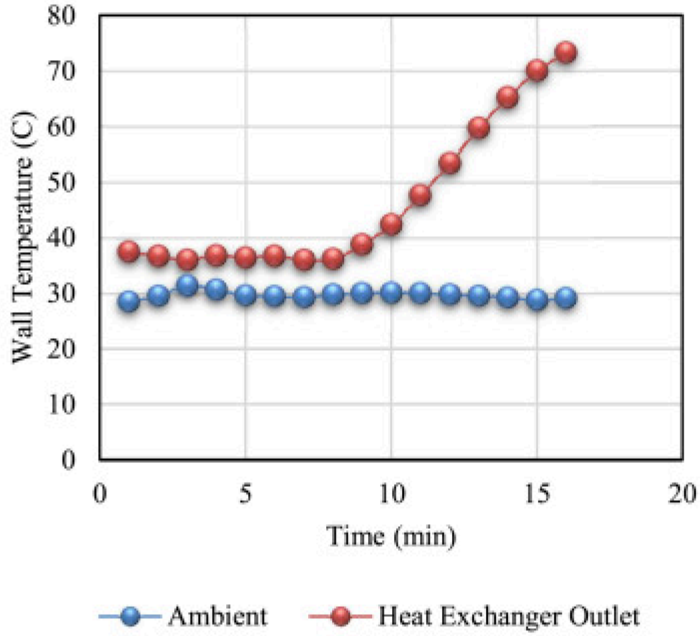

Wall Temperature (C)
Time (min)
Ambient
Heat Exchanger Outlet

(a)

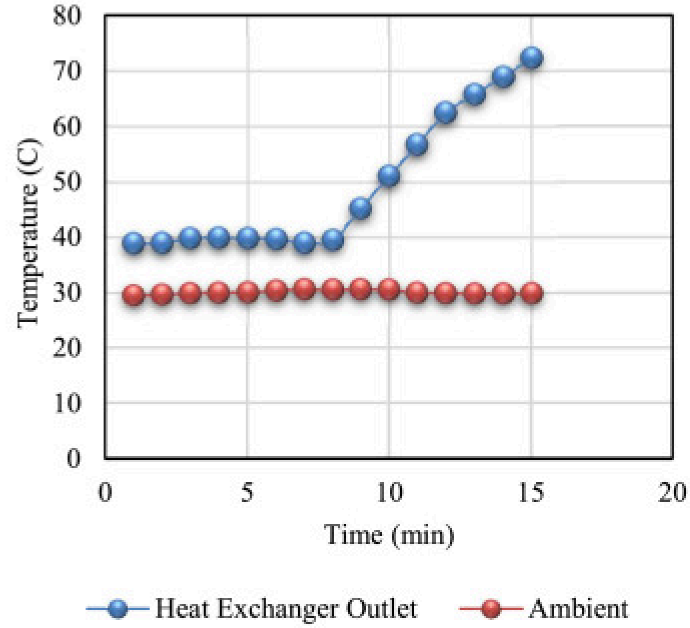

Temperature (C)
Time (min)
Heat Exchanger Outlet
Ambient

(b)

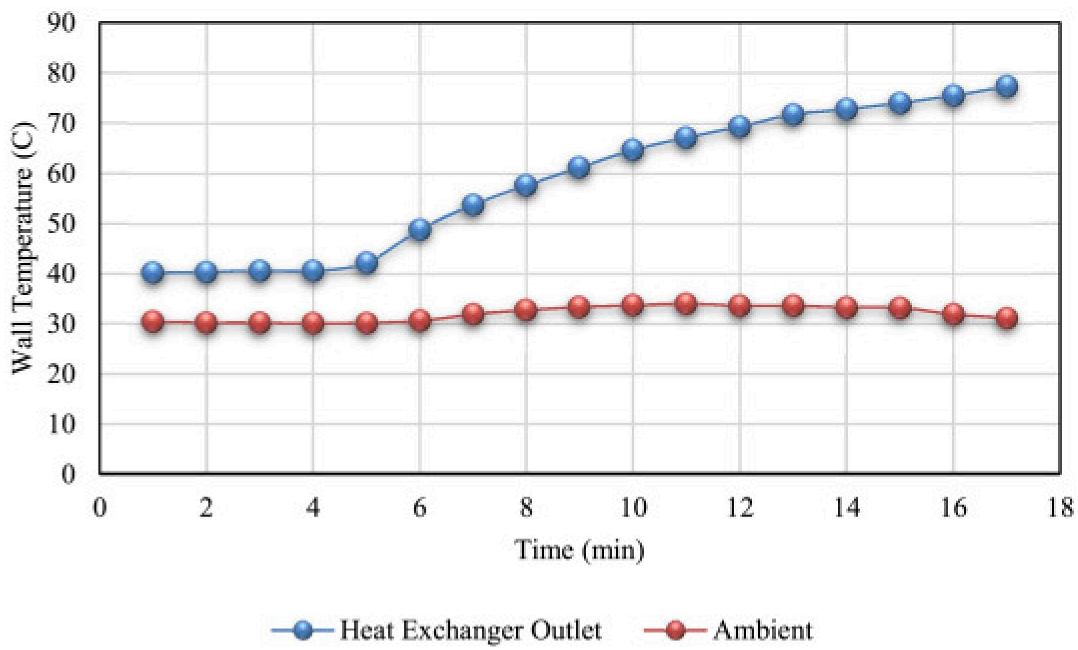

Wall Temperature (C)
Time (min)
Heat Exchanger Outlet
Ambient

(c)

Download: Download high-res image (704KB)

Download: Download full-size image

Fig. 9. Variation of inlet and outlet temperature of air in the heat exchanger during heating process via time for volume flow rate as a)10 $mL \cdot s^{-1}$, b) 14 $mL \cdot s^{-1}$, and c) 33 $mL \cdot s^{-1}$.

This presents a critical design trade-off: while higher flow rates minimize thermal inertia and accelerate system response, they yield lower temperature lift on the air side. Downstream applications requiring either rapid thermal response or high-temperature output must navigate this trade-off, which is quantitatively characterized by the time constant data. The most dynamic response was observed at the highest tested flow rate of 33 $mL \cdot s^{-1}$, where the outlet air temperature rose very sharply reaching its near-steady-state value in the shortest time as a direct consequence of the reduced receiver time constant, while the air-side temperature differential stabilized at a lower value of approximately 3 °C consistent with the fundamental heat exchanger principle that for a given heat load, a higher mass flow rate results in smaller temperature changes. The data confirms that while higher oil flow rates minimize receiver thermal inertia and lead to faster system response, they also result in lower temperature lift on the air side of the heat exchanger, presenting a critical trade-off for system integration where downstream applications may require either rapid thermal response or high-temperature output.

4.3.2. Thermal decay

Following radiation cessation (Fig. 10), both inlet and outlet air temperatures exhibited exponential decay consistent with first-order response. At 10 $mL \cdot s^{-1}$, the decline was relatively gradual, as slower-moving oil had longer residence time releasing stored thermal energy over extended periods. At 33 $mL \cdot s^{-1}$, the air outlet temperature demonstrated steeper and more rapid decline, as higher mass flow rate transported thermal energy more quickly but also led to faster depletion of available thermal mass upon energy source removal.

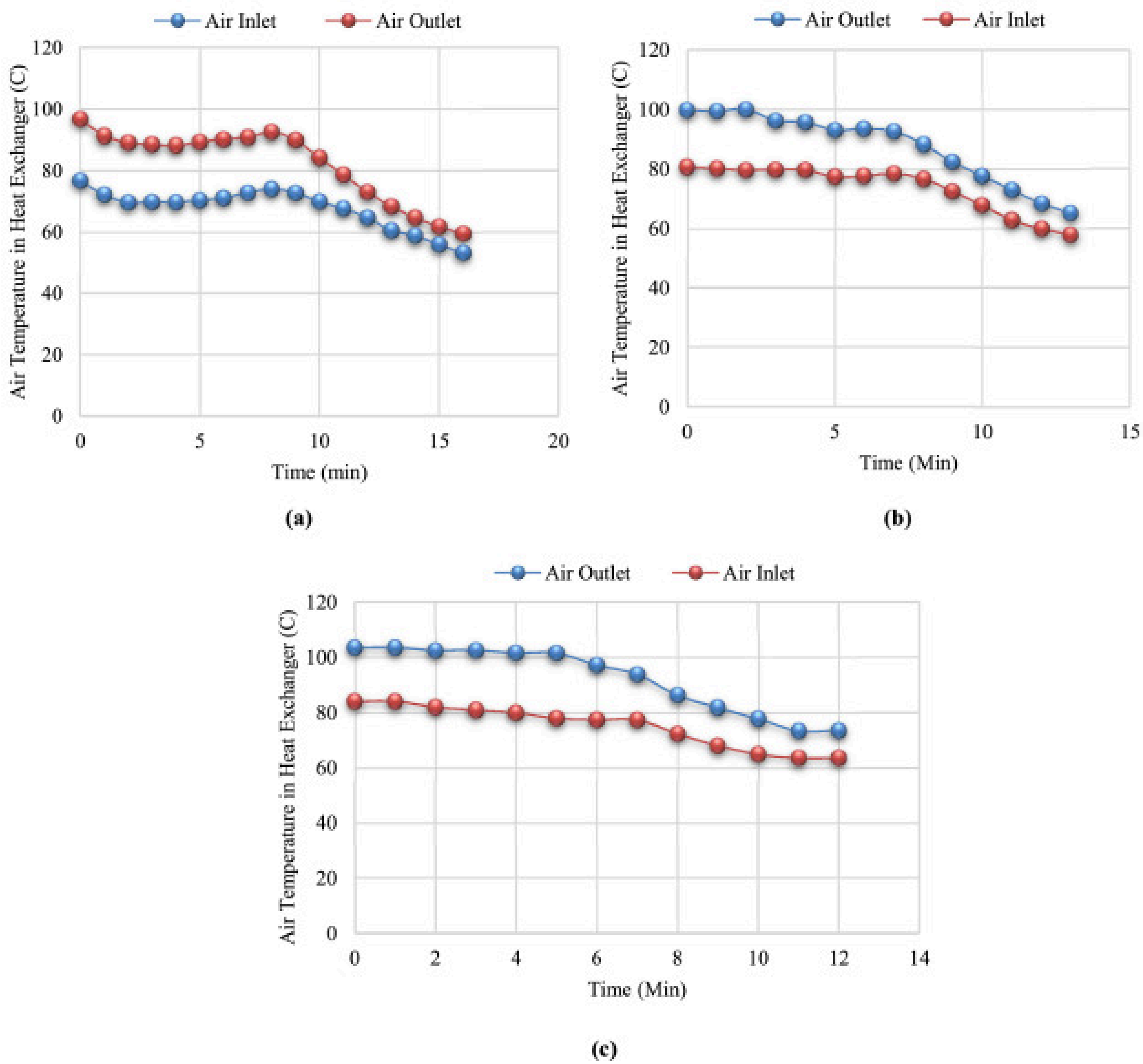

Download: Download high-res image (474KB)

Download: Download full-size image

Fig. 10. Variation of inlet and outlet temperature of air in the heat exchanger during thermal decay process via time for volume flow rate as a)10 $mL{\cdot}s^{-1}$, b) 14 $mL{\cdot}s^{-1}$, and c) 33 $mL{\cdot}s^{-1}$.

The temperature difference ΔT_{air} was maximum at thermal decay onset, reflecting high thermal energy content of oil exiting the receiver, subsequently diminishing toward zero as the system reached thermal equilibrium. The rate at which ΔT_air approached zero directly indicated the system's overall thermal time constant, confirming that higher flow rates accelerate equilibration. This finding carries importance for grid operators: faster thermal response facilitated by higher flow rates enables more agile thermal energy management, allowing better anticipation and mitigation of solar intermittency effects.

4.4. Solar radiation intensity and optical efficiency analysis

To provide a comprehensive characterization of the hemispherical cavity receiver performance, the solar radiation intensity and optical efficiency of the system were analyzed alongside the transient thermal behavior. The Direct Normal Irradiance (DNI) was continuously monitored using a calibrated pyranometer mounted on the tracking structure throughout all experimental tests. Table 10 presents the temporal variation of solar radiation intensity during representative heating and cooling tests for the three flow rate conditions.

Table 10. Solar radiation intensity (DNI) variation during experimental tests.

Time (min)	DNI at 10 ml/s (W/m^2)	DNI at 14 ml/s (W/m^2)	DNI at 33 ml/s (W/m^2)
0	720	740	760
2	745	765	790
4	770	785	810
6	785	800	830
8	800	815	845
10	810	825	855
12	820	835	860
14	825	840	858

Time (min)	DNI at 10 ml/s (W/m²)	DNI at 14 ml/s (W/m²)	DNI at 33 ml/s (W/m²)
16	830	838	855
18	828	835	850
20	825	830	845

The solar radiation intensity remained relatively stable during each test period, with fluctuations of <8% from the mean value, ensuring consistent boundary conditions for time constant determination (Table 11). The average DNI values varied slightly across different test days, ranging from 790 W/m² at the lowest flow rate condition to 830 W/m² at the highest flow rate condition, attributable to normal diurnal and seasonal variations in solar irradiance.

Table 11. Solar radiation conditions and receiver effectiveness parameters.

Parameter	Value	Notes
DNI range	720–860 W/m²	Measured during tests
Average DNI (10 ml/s)	790 ± 35 W/m²	During heating phase
Average DNI (14 ml/s)	808 ± 30 W/m²	During heating phase
Average DNI (33 ml/s)	830 ± 28 W/m²	During heating phase
Reflector optical efficiency	0.84	Manufacturer specification
Receiver absorptivity	0.97	Black chrome coating
Receiver optical effectiveness	84.2%	Calculated from measured parameters
Thermal effectiveness (10 ml/s)	67.5%	Steady-state condition
Thermal effectiveness (14 ml/s)	71.8%	Steady-state condition

Parameter	Value	Notes
Thermal effectiveness (33 ml/s)	76.2%	Steady-state condition
Average wind speed	1.2–2.5 m/s	Measured during tests
Ambient temperature	28–32 °C	Measured during tests

4.5. Operationalizing energy governance: A framework for experimental data integration

To establish a measurable and direct link between the experimental findings and the objectives of energy governance, an operational framework is presented that translates technical parameters into actionable governance indicators. This framework operationalizes the concept of energy governance by defining specific metrics derived from our experimental data, as presented in Table 12.

Table 12. Operational framework linking experimental parameters to energy governance objectives.

Governance Dimension	Technical Parameter	Defined Indicator	Policy/Governance Application
Regulatory Governance	Time Constant (τ)	A system's dynamic responsiveness (e.g., $\tau_{heating}$=0.82 min)	Establishing minimum dynamic performance standards for collector certification and grid interconnection codes.
Financial Governance	Flow-Rate Sensitivity ($\Delta\tau/\Delta\dot{V}$)	A system's controllability and predictability (e.g., 23.8% improvement in $\tau_{heating}$ from 10 to 33 $mL{\cdot}s^{-1}$)	De-risking technology for investors, enabling accurate energy yield modeling, and informing performance-based incentives.

Governance Dimension	Technical Parameter	Defined Indicator	Policy/Governance Application
Strategic Governance	Heating/Thermal decay Asymmetry ($\tau_{thermal\ decay}/\tau_{heating}$)	A system's resilience and storage integration potential (e.g., ratio of 2.6–3.0)	Informing R&D priorities, technology roadmaps, and public funding allocation for thermal storage and control systems.
Sustainability Governance	Thermal decay Time Constant ($\tau_{thermal\ decay}$)	A system's response to solar intermittency (e.g., $\tau_{thermal\ decay}$=2.16 min at 33 $mL·s^{-1}$)	Enhancing grid stability, optimizing reserve capacity management, and reducing reliance on fossil-fuel backup.

By defining these indicators, the experimental data no longer remain purely technical metrics but become foundational inputs for an evidence-based governance approach. For instance, the experimentally determined heating time constants ($\tau_{heating}$=0.82 min at 33 $mL·s^{-1}$ and 1.078 min at 10 $mL·s^{-1}$) provide a quantifiable basis for regulatory bodies to propose a maximum allowable τ for systems seeking priority grid access. Similarly, the quantified thermal decay time constants (2.16–3.16 min) offer precise parameters for grid operators to model system behavior during cloud cover events, directly informing the operational protocols that constitute the implementation of energy governance."

4.6. Improving energy governance: implications of experimental findings

The experimental quantification of the hemispherical cavity receiver's transient thermal behavior, combined with the analysis of solar radiation intensity and optical/thermal effectiveness, provides foundational empirical evidence that directly strengthens multiple dimensions of energy governance through the operationalized framework defined in the previous section. The time constant values derived from heating and thermal decay processes, ranging from 0.82 to 1.078 min during heating and 2.16 to 3.16 min during thermal decay across volumetric flow rates of 10 to 33 $mL·s^{-1}$, constitute critical performance benchmarks that transcend technical characterization to serve as actionable intelligence for policymakers, grid operators, and financial institutions. Additionally, the quantified optical effectiveness (84.2%) and thermal effectiveness (67.5–76.2%) provide comprehensive performance metrics for system evaluation. These experimentally validated parameters address the fundamental governance challenge of uncertainty reduction, transforming solar thermal systems from variable black-box technologies into predictable energy assets whose dynamic behavior can be integrated into national energy planning frameworks.

The inverse relationship between volumetric flow rate and thermal time constant carries profound implications for regulatory governance and technical standard development. The reduction in heating time constant from 1.078 min at 10 $mL·s^{-1}$ to 0.82 min at 33 $mL·s^{-1}$, accompanied by corresponding thermal decay improvements from 3.16 to 2.16 min, establishes quantifiable design parameters that can be codified into testing protocols for concentrated solar power components. Regulatory bodies responsible for collector certification and grid connection codes can leverage these experimentally derived relationships to develop evidence-based standards specifying minimum dynamic performance requirements, ensuring deployed systems possess the thermal responsiveness necessary for stable grid integration. The rigorous outdoor testing methodology provides a replicable framework strengthening the technical capacity of regulatory institutions to create credible, enforceable standards.

From the perspective of financial governance and investment mobilization, the empirical characterization of receiver dynamics directly addresses the technology risk perception that historically constrains private capital flow into concentrated solar power projects. The availability of validated time constant data enables project developers and financial analysts to construct more accurate energy yield models accounting for transient behavior during cloud cover events and startup sequences. Unlike steady-state efficiency metrics assuming idealized continuous operation, the dynamic parameters reported permit realistic simulation of annual energy production under actual solar radiation variability, thereby reducing uncertainty in financial projections and improving project bankability. The thermal decay time constant data provides essential information for designing thermal energy storage integration strategies, as the rate of thermal energy loss during radiation intermittency directly influences storage sizing and dispatchability guarantees. By de-risking these technical uncertainties, the research facilitates more precise power purchase agreements and accelerates private capital mobilization toward renewable energy infrastructure.

The strategic governance dimension of national technology roadmapping finds direct empirical support in the comparative analysis of transient thermal behavior across operating conditions. The demonstrated sensitivity of the time constant to fluid flow rate provides evidence-based guidance for public research funding allocation and technology development strategies.

Policymakers can utilize these findings to justify investment in advanced control systems and variable-speed pumping infrastructure that leverage the responsiveness of optimized cavity receiver designs. Furthermore, the experimental methodology serves as a template for national laboratories seeking to generate comparable performance data for locally manufactured collector systems, building indigenous technical capacity and reducing dependence on foreign technology certifications.

The sustainability governance imperative of accelerating the low-carbon transition while ensuring grid reliability is directly advanced by the enhanced understanding of solar thermal system dynamics. Grid operators require precise knowledge of how distributed generation assets respond to solar radiation fluctuations, and the time constant values reported enable the development of predictive control algorithms that anticipate output variations, allowing more efficient reserve capacity management and reduced reliance on fossil-fuel backup. The thermal decay phase data informs load management strategies during cloud transients, providing grid controllers with temporal parameters necessary to coordinate complementary generation sources, thereby directly contributing to energy security objectives.

Finally, the science-policy interface essential for effective energy governance is strengthened through the translation of complex thermal dynamic data into accessible performance metrics. The time constant, as a single comprehensive parameter encapsulating system thermal inertia, provides an intuitive yet technically rigorous indicator communicable to policymakers and investors without requiring specialized engineering expertise. This study's demonstration of how fundamental thermal-fluid science generates actionable governance-relevant knowledge exemplifies the bidirectional information flow necessary for evidence-based energy policy, bridging the gap between laboratory research and real-world energy system management to enable targeted policies and investment incentives that accelerate deployment of reliable solar thermal technologies. Summary of improving energy governance using developing the current experimental tests is presented in Fig. 11.

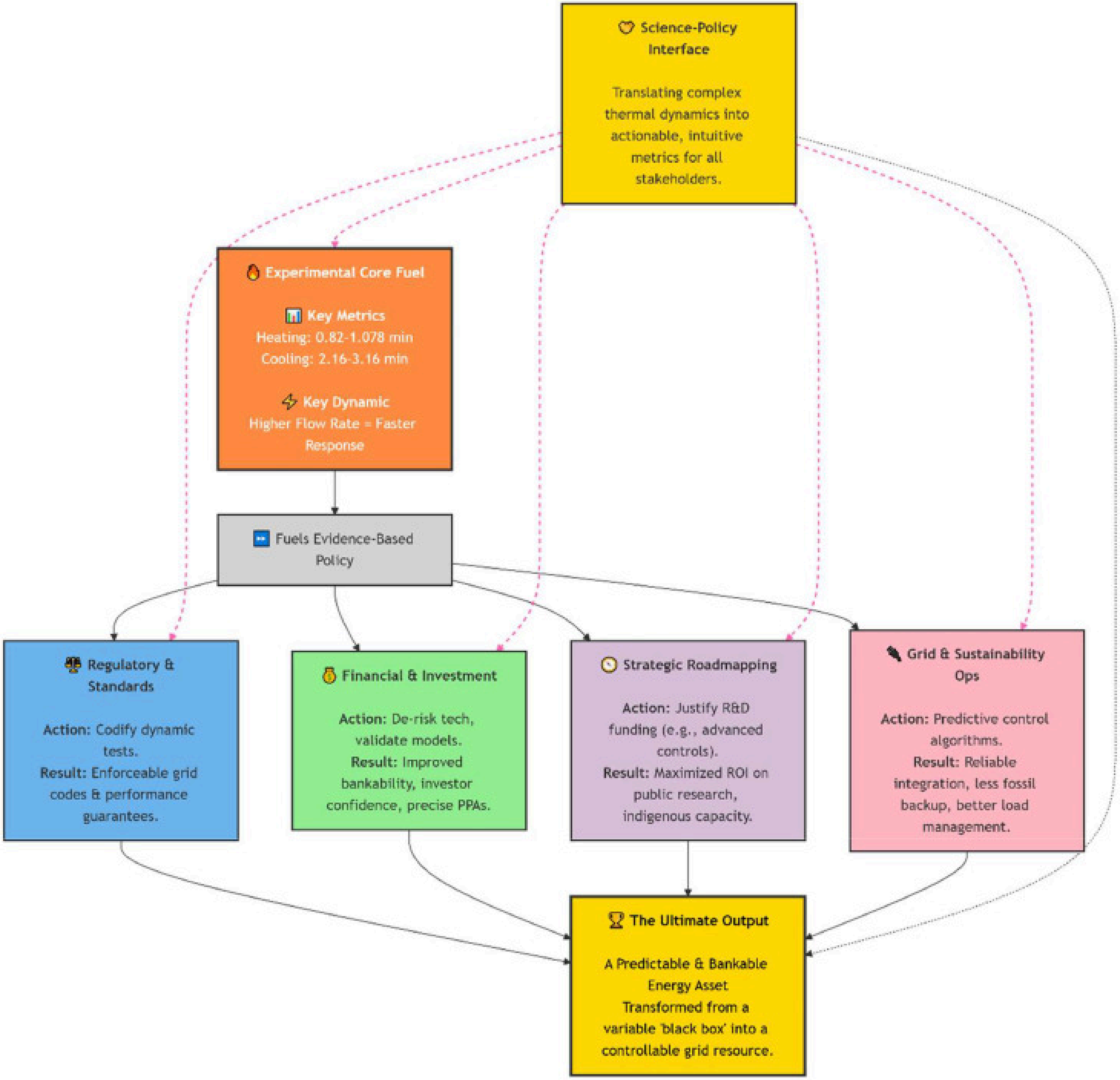

Science-Policy Interface
Translating complex thermal dynamics into actionable, intuitive metrics for all stakeholders.
Experimental Core Fuel
Key Metrics
Heating: 0.82-1.078 min
Cooling: 2.16-3.16 min
Key Dynamic
Higher Flow Rate = Faster Response
Fuels Evidence-Based Policy
Regulatory & Standards
Action: Codify dynamic tests.
Result: Enforceable grid codes & performance guarantees.
Financial & Investment
Action: De-risk tech, validate models.
Result: Improved bankability, investor confidence, precise PPAs.
Strategic Roadmapping
Action: Justify R&D funding (e.g., advanced controls).
Result: Maximized ROI on public research, indigenous capacity.
Grid & Sustainability Ops
Action: Predictive control algorithms.
Result: Reliable integration, less fossil backup, better load management.
The Ultimate Output
A Predictable & Bankable Energy Asset
Transformed from a variable 'black box' into a controllable grid resource.

Download: Download high-res image (799KB)

Download: Download full-size image

Fig. 11. Summary of improving energy governance using developing the current experimental tests.

4.7. Policy making: translating experimental insights into actionable energy strategies

The empirical findings from this experimental investigation into the transient thermal behavior of a hemispherical cavity receiver establish a robust scientific basis for formulating evidence-based energy policies designed to accelerate concentrated solar power deployment. The quantified time constant values, ranging from 0.82 to 1.078 min during heating and 2.16 to 3.16 min during thermal decay across flow rates of 10 to 33 $mL{\cdot}s^{-1}$, transcend their technical significance to serve as critical inputs for policy development across multiple governance levels. These experimentally validated parameters address the fundamental challenge of bridging laboratory research and commercial deployment, providing policymakers with empirical evidence necessary to design targeted interventions that simultaneously promote technological innovation, ensure grid reliability, and advance national energy security objectives.

The establishment of performance-based standards and certification protocols for solar thermal collectors emerges as a primary policy recommendation from this investigation. Regulatory frameworks currently rely heavily on steady-state efficiency metrics that fail to capture dynamic behavior critical for grid integration, whereas the time constant methodology demonstrated herein offers a replicable testing protocol that can be codified into national and international standards. Mandating transient response characterization as a mandatory performance indicator in collector certification would ensure deployed systems possess the thermal responsiveness necessary for stable grid operation while creating standardized benchmarks for meaningful comparison across different receiver geometries, working fluids, and manufacturing approaches, ultimately strengthening renewable energy governance through enhanced market transparency and consumer protection.

The demonstrated inverse relationship between volumetric flow rate and thermal time constant carries direct implications for financial incentive mechanisms and tariff structures. Feed-in tariffs, renewable energy certificates, and investment tax credits typically differentiate support based on installed capacity or estimated annual production without accounting for dynamic performance characteristics that determine actual grid value. The experimental data revealing that higher flow rates yield faster thermal response—with heating time constant improving from 1.078 min at 10 $mL{\cdot}s^{-1}$ to 0.82 min at 33

$mL \cdot s^{-1}$—provides evidence-based rationale for tiered incentive structures rewarding superior dynamic performance. Incorporating time constant thresholds into eligibility criteria for enhanced financial support would create market signals encouraging adoption of optimized receiver designs, advanced control systems, and variable-speed pumping infrastructure, maximizing societal return on public investment while promoting technological innovation.

Strategic allocation of public research and development funding represents another critical policy dimension informed by this investigation. National energy technology roadmaps require empirical evidence to identify promising technical pathways, yet funding decisions are frequently guided by theoretical potential rather than demonstrated real-world performance. The experimental quantification of time constant sensitivity to operating parameters provides concrete data for prioritizing research directions that yield measurable improvements in system responsiveness, supporting increased investment in advanced control algorithms, variable-speed pumping systems, and thermal energy storage integration strategies. Furthermore, the successful experimental methodology serves as a template for publicly funded research programs seeking to generate comparable performance data, ensuring future policy decisions are grounded in rigorous empirical evidence.

Grid integration policies and interconnection standards for distributed solar thermal generation require substantial revision based on the characterized transient behavior. Current grid codes specify steady-state power quality requirements but lack provisions addressing thermal inertia characteristics that determine system response to solar radiation variability. The time constant data, particularly thermal decay phase values ranging from 2.16 to 3.16 min, provide quantifiable parameters for predicting system behavior during cloud cover events and developing appropriate reserve capacity requirements. Mandating time constant characterization in grid impact assessments would enable system operators to evaluate cumulative effects on stability, while recognizing fast-response solar thermal systems as eligible providers of ancillary services would create revenue streams rewarding demonstrated dynamic performance advantages.

The international dimension of energy governance encompassing technology transfer, capacity building, and standards harmonization finds direct relevance in this study's policy implications. Developing economies with abundant solar resources frequently lack the technical infrastructure and regulatory capacity to evaluate competing technologies and establish appropriate performance standards. The experimentally validated methodology and resulting time constant data provide a transferable knowledge base for capacity building initiatives targeting regulatory institutions in emerging economies, while supporting international harmonization of testing standards that reduces trade barriers and facilitates technology transfer through common performance metrics recognized across national jurisdictions.

Finally, integrating experimental research outcomes into policy formulation requires institutional mechanisms facilitating sustained science-policy dialogue. Translating technical parameters such as the time constant into accessible policy-relevant indicators demands ongoing collaboration between research institutions, regulatory agencies, and industry associations. Establishing formal advisory mechanisms including technical working groups and standing committees ensures continuous incorporation of emerging research findings into policy development processes. This experimental investigation exemplifies rigorous, policy-relevant research demonstrating that fundamental thermal-fluid science generates actionable knowledge directly applicable to energy transition governance challenges, and institutionalizing these science-policy linkages ensures renewable energy policies remain grounded in empirical evidence, responsive to technological advancements, and capable of achieving accelerated deployment while ensuring system reliability and economic efficiency. Relation between the results of the current experimental tests and policy making is presented in Fig. 12.

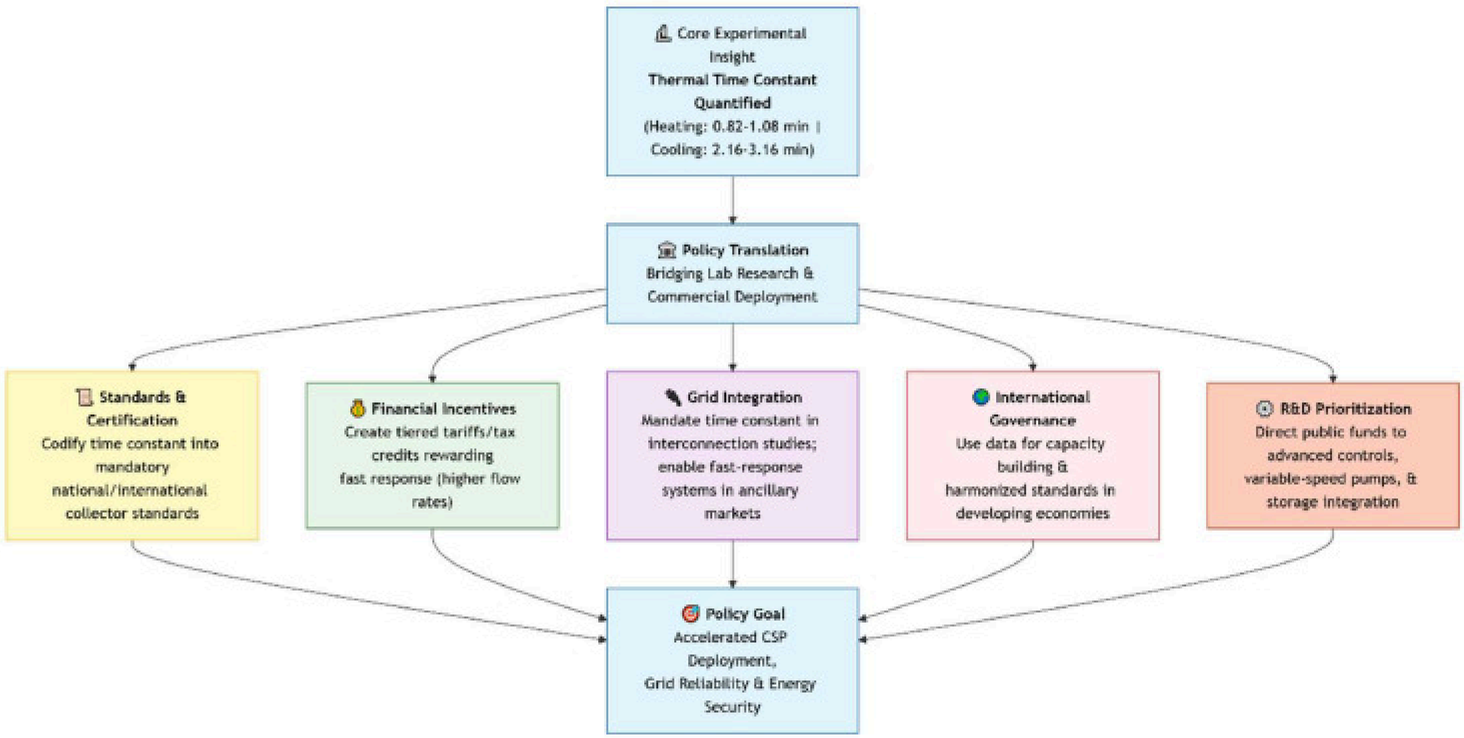

Download: Download high-res image (436KB)

Download: Download full-size image

Fig. 12. Relation between the results of the current experimental tests and policy making.

4.8. Recommended policies: translating experimental findings into actionable governance frameworks

The experimental quantification of the hemispherical cavity receiver's transient thermal behavior—with time constants of 0.82–1.078 min during heating and 2.16–3.16 min during thermal decay across flow rates of 10–33 $mL\cdot s^{-1}$—provides empirical evidence for targeted policy interventions. Building on the operationalized governance framework presented in this study, these scientifically derived parameters enable evidence-based governance frameworks addressing technical, economic, and regulatory dimensions of solar thermal deployment. For each policy recommendation below, we explicitly link the recommendation to the specific experimental data that supports it and define how it operationalizes a dimension of energy governance.

Establishment of Dynamic Performance Standards for Solar Thermal Certification

- National regulatory bodies should mandate time constant characterization as a mandatory performance indicator in collector certification protocols, complementing steady-state efficiency requirements with transient response metrics reflecting real-world operating conditions

- The experimentally validated methodology for determining heating and thermal decay time constants should be codified into national and international testing standards (ISO/IEC frameworks) to ensure consistent performance evaluation across different receiver geometries, working fluids, and manufacturing approaches

- Certification thresholds should be established based on empirical data, with maximum acceptable heating time constants of 1.5 min and thermal decay time constants of 3.5 min at reference flow rates to ensure thermal responsiveness necessary for stable grid integration

- Regular review and updating of these standards should be mandated to incorporate technological advancements, with the presented methodology serving as a replicable template for future standard development

Performance-Based Financial Incentive Structures

- Feed-in tariffs and renewable energy certificate programs should incorporate time constant thresholds into tiered incentive structures, with systems demonstrating heating time constants below 1.0 min at 33 $mL \cdot s^{-1}$ qualifying for premium tariff rates reflecting enhanced grid integration value

- Investment tax credits and capital subsidies should differentiate support levels based on dynamic performance, with higher incentive rates applied to systems incorporating variable-speed pumping infrastructure and advanced control algorithms that optimize thermal response across varying solar conditions

- Green banking and concessional financing programs should integrate time constant performance into project eligibility criteria and interest rate determinations, recognizing that superior transient response characteristics present reduced technical risk and improved bankability
- Demonstration projects showcasing optimal flow rate strategies (33 $mL{\cdot}s^{-1}$ yielding fastest thermal response) should receive priority access to public funding mechanisms to accelerate market adoption of high-performance configurations

Grid Integration and Interconnection Policy Reforms

- Grid interconnection standards for distributed solar thermal generation should require time constant characterization as part of interconnection studies, enabling evaluation of cumulative impact on grid stability during solar radiation fluctuations
- System impact assessments should mandate submission of experimentally validated time constant data for proposed projects, with minimum dynamic performance requirements of heating time constants below 1.2 min and thermal decay time constants below 3.0 min at design flow rates
- Grid codes should recognize fast-response solar thermal systems as eligible providers of ancillary services including frequency regulation and ramp management, with compensation mechanisms reflecting the demonstrated value of rapid thermal response
- Distribution system operators should develop forecasting protocols incorporating time constant parameters for accurate prediction of output variations during cloud cover events based on quantified thermal decay rates of 2.16–3.16 min

Research and Development Funding Prioritization

- Public research funding agencies should prioritize investments in advanced control algorithms capable of real-time flow rate modulation based on solar radiation forecasts, leveraging the demonstrated relationship between flow rate and thermal response

- Funding programs should support development of variable-speed pumping systems maintaining optimal flow rates across varying conditions, recognizing that 33 $mL \cdot s^{-1}$ yields 23.8% faster heating response compared to 10 $mL \cdot s^{-1}$
- Research initiatives on thermal energy storage integration should utilize experimentally characterized thermal decay dynamics to optimize storage sizing and dispatchability strategies, particularly the 2.16-minute thermal decay constant at maximum flow rate
- International collaboration programs should fund technology transfer and capacity building initiatives disseminating experimental methodology and time constant characterization techniques to developing economies with significant solar resources

Market Development and Industry Support Mechanisms

- Technology demonstration programs should showcase systems achieving optimal time constant performance, creating visible market examples demonstrating the value proposition of fast-response solar thermal technology
- Industry training and workforce development initiatives should incorporate time constant characterization techniques and dynamic performance optimization strategies into curriculum for engineers, installers, and system operators
- Export promotion programs should prioritize support for manufacturers whose systems demonstrate validated time constant performance meeting or exceeding international standards
- Public procurement policies for government facilities should mandate minimum dynamic performance requirements aligned with experimental findings, creating anchor demand for high-performance systems

Regulatory Framework Enhancements

- Building energy codes should include provisions for solar thermal system dynamic performance, with time constant requirements integrated into compliance pathways for renewable energy contributions
- Environmental impact assessment guidelines should require consideration of system dynamic behavior in evaluating grid stability implications and contribution to reliable renewable energy supply
- Utility resource planning regulations should mandate that integrated resource plans account for temporal characteristics of solar thermal generation using time constant data to model system behavior
- Consumer protection regulations should require disclosure of time constant performance in product labeling, enabling informed purchasing decisions based on comprehensive metrics beyond steady-state efficiency

International Cooperation and Standard Harmonization

- National standards bodies should actively participate in international forums (ISO, IEC) to advance harmonization of time constant testing protocols, ensuring the validated methodology contributes to globally recognized standards
- Bilateral and multilateral technology cooperation agreements should include provisions for sharing experimental methodologies and performance data to accelerate global diffusion of best practices
- Development assistance programs for renewable energy in emerging economies should incorporate technical assistance for establishing time constant testing capabilities
- International trade agreements should recognize harmonized time constant standards as legitimate technical regulations, reducing non-tariff barriers while ensuring imported technologies meet minimum dynamic performance requirements

These policy recommendations, grounded in experimentally validated time constant data, provide a comprehensive framework for translating technical research into actionable governance mechanisms. Integrating dynamic performance considerations into certification standards, financial incentives, grid codes, and research priorities enables policymakers to accelerate deployment of solar thermal systems that achieve both high steady-state efficiency and transient response characteristics essential for reliable grid integration and optimal energy system performance.

5. Conclusions and policy implications

This experimental investigation successfully characterized the transient thermal behavior of a hemispherical cavity receiver integrated with a solar dish concentrator using pure thermal oil as the heat transfer fluid, establishing critical empirical benchmarks for system dynamic performance. The time constant methodology applied under real outdoor conditions during both heating and thermal decay processes yielded quantifiable parameters that elucidate the receiver's thermal inertia and its dependence on operational variables. Furthermore, the analysis of solar radiation intensity (DNI: 720–860 W/m^2), optical effectiveness (84.2%), and thermal effectiveness (67.5–76.2%) provides a comprehensive performance characterization. The findings demonstrate that the hemispherical cavity receiver exhibits first-order thermal response characteristics, with time constant values inversely proportional to volumetric flow rate, ranging from 0.82 to 1.08 min during heating and 2.16 to 3.16 min during thermal decay across flow rates of 10 to 33 $mL{\cdot}s^{-1}$. Increasing flow rate from 10 $mL{\cdot}s^{-1}$ to 33 $mL{\cdot}s^{-1}$ reduced heating time constant by 23.8% and thermal decay time constant by 31.6%. Thermal decay time constants were consistently 2.6 to 3.0 times larger than heating constants across all flow rates, indicating that thermal energy dissipation occurs more slowly than energy absorption. High coefficients of determination (R^2 ranging from 0.962 to 0.999) confirmed the receiver follows first-order exponential behavior, validating the time constant as a robust metric for characterizing system dynamic performance. The thermal effectiveness improved with increasing flow rate from 67.5% to 76.2%, confirming that higher flow rates enhance both transient and steady-state performance. Heat exchanger measurements confirmed effective energy transfer, with air-side temperature differential decay rates consistent with oil-side time constants. These experimentally validated parameters provide the foundational data necessary for developing predictive control algorithms, optimizing system design, and establishing performance standards that enhance the reliability and grid integration capability of concentrated solar power technologies. Most important findings can be summarized as following:

- **Flow rate dependence of thermal response**: Increasing volumetric flow rate from 10 ml/s to 33 ml/s reduced the heating time constant by 23.8% (from 1.078 to 0.82 min) and the cooling time constant by 31.6% (from 3.16 to 2.16 min), demonstrating that higher flow rates significantly accelerate system thermal response and reduce thermal inertia.

- **Asymmetry between heating and cooling dynamics**: Cooling time constants were consistently 2.6 to 3.0 times larger than corresponding heating time constants across all flow rates, indicating that thermal energy dissipation occurs more slowly than energy absorption—a critical parameter for predicting system behavior during cloud cover events and designing thermal energy storage integration strategies.

- **Experimental validation of first-order thermal model:** The high coefficients of determination (R^2 ranging from 0.9623 to 0.9988) confirmed that the hemispherical cavity receiver closely follows first-order exponential behavior during both heating and cooling transients, validating the time constant as a robust metric for characterizing system dynamic performance.

- **Heat exchanger performance validation:** The air temperature differential across the heat exchanger during cooling exhibited decay rates consistent with the oil-side time constants, confirming effective energy transfer and validating the integrated system's thermal response characteristics.

- **Solar radiation and effectiveness analysis:** DNI remained stable within 8% variation during each test, with optical effectiveness of 84.2% and thermal effectiveness ranging from 67.5% to 76.2%, demonstrating that the receiver effectively converts concentrated solar radiation into thermal energy with performance comparable to previous studies.

The experimentally validated parameters provide foundational data for developing predictive control algorithms, optimizing system design, and establishing performance standards that enhance renewable energy reliability. From a governance perspective, these findings enable evidence-based policy development by providing quantifiable benchmarks for collector certification standards, performance-based financial incentives that reward fast-response systems, and grid interconnection requirements ensuring stable integration of solar thermal generation. The demonstrated relationship between flow rate and thermal response supports strategic investment in variable-speed pumping systems and advanced control strategies, while the quantified transient response data reduces technology risk perception for project financiers and grid operators. By establishing rigorous empirical benchmarks, this research strengthens the science-policy interface and accelerates the transition toward reliable, low-carbon energy systems. Future research should extend this methodology to evaluate nanofluid-enhanced working fluids and investigate receiver geometric parameter effects on transient response. More important polices can be presented as following:

- **Regulatory governance contribution:** The experimentally validated time constant methodology provides a replicable testing protocol that can be codified into national and international certification standards, enabling regulatory bodies to establish minimum dynamic performance requirements that ensure deployed systems possess the thermal responsiveness necessary for reliable grid operation.

- **Financial governance contribution:** The availability of empirically derived transient response data reduces technology risk perception by enabling accurate energy yield modeling under realistic solar variability conditions, improving project bankability and facilitating private capital mobilization for renewable energy infrastructure development.

- **Strategic governance contribution:** The demonstrated relationship between flow rate and thermal response provides evidence-based guidance for public research funding allocation, supporting investment in variable-speed pumping systems, advanced control algorithms, and thermal energy storage integration strategies that maximize system performance and grid integration capability.

- **Sustainability governance contribution:** Enhanced understanding of system dynamic behavior enables grid operators to manage solar thermal generation more effectively, reducing reliance on fossil-fuel backup and accelerating the transition toward reliable, low-carbon energy systems.

This investigation conclusively demonstrates that experimental time constant analysis constitutes an indispensable tool for advancing both the technical performance of solar thermal systems and the governance frameworks necessary for their widespread deployment. The empirical data generated herein bridge the critical gap between laboratory research and real-world energy system management, providing policymakers, regulators, investors, and grid operators with the quantitative foundation required for informed decision-making. Future research should extend this methodology to evaluate nanofluid-enhanced working fluids, investigate the influence of receiver geometric parameters on transient response, and develop predictive control algorithms that leverage time constant characterization to optimize system performance under fluctuating solar radiation conditions. Furthermore, the economic implications of the quantified transient behavior—including the impact of time constant reduction on system sizing, thermal storage requirements, and grid integration costs—represent a critical avenue for future investigation. A comprehensive techno-economic analysis incorporating the experimentally validated time constant data reported herein would provide valuable insights for project developers and financial institutions, thereby strengthening the evidence base for investment decisions in concentrated solar power technologies. By continuing to strengthen the empirical basis for solar thermal technology deployment, such investigations will further advance the institutional capacity for evidence-based energy governance and accelerate the global transition toward sustainable, secure, and resilient energy systems.

Declaration of AI use / acknowledgment of AI assistance

The authors confirm that all scientific content—including raw data, statistical analyses, and result interpretations—was generated entirely by the authors without the use of generative artificial intelligence. AI tools were employed exclusively for language polishing, grammar correction, and clarity improvements of the authors' own findings. The authors bear full responsibility for the integrity and originality of the work.

CRediT authorship contribution statement

Reyhaneh Loni: Writing – review & editing, Writing – original draft, Validation, Software, Methodology, Investigation, Formal analysis. **Ezzatollah Askari Asli-Ardeh:** Supervision, Project administration, Funding acquisition. **Barat Ghobadian:** Supervision, Project administration, Funding acquisition, Conceptualization.

Declaration of competing interest

There is no conflict of interest.

Recommended articles

Data availability

Data will be made available on request.

References

[1] J. Du, Z. Shen, M. Song, M. Vardanyan
The role of green financing in facilitating renewable energy transition in China: perspectives from energy governance, environmental regulation, and market reforms
Energy Econ., 120 (2023), Article 106595
View PDF View article View in Scopus ↗ Google Scholar ↗

[2] A.M. Moghani, R. Loni
Review on energy governance and demand security in oil-rich countries
Energy Strat. Rev., 57 (2025), Article 101625
View PDF View article View in Scopus ↗ Google Scholar ↗

[3] M. Sharifzadeh, R. Loni
Performance of a solar parabolic trough concentrator using vacuum linear V-shaped cavity receiver
Therm. Sci. Eng. Prog., 51 (2024), Article 102609
View PDF View article View in Scopus ↗ Google Scholar ↗

[4] K. Shahverdi, E. Bellos, R. Loni, G. Najafi, Z. Said
Solar-driven water pump with organic rankine cycle for pressurized irrigation systems: a case study
Therm. Sci. Eng. Prog., 25 (2021), Article 100960
View PDF View article View in Scopus ↗ Google Scholar ↗

[5] A. Arkian, G. Najafi, S. Gorjian, R. Loni, E. Bellos, T. Yusaf

Performance assessment of a solar dryer system using small parabolic dish and alumina/oil nanofluid: simulation and experimental study
Energies, 12 (2019), p. 4747
Article
Crossref ↗ View in Scopus ↗ Google Scholar ↗

[6] S. Pavlovic, R. Loni, E. Bellos, D. Vasiljević, G. Najafi, A. Kasaeian
Comparative study of spiral and conical cavity receivers for a solar dish collector
Energy Convers. Manage., 178 (2018), pp. 111-122
View PDF View article View in Scopus ↗ Google Scholar ↗

[7] A. Rafiei, R. Loni, M.H. Ahmadi, G. Najafi, E. Bellos, F. Rajaee, E.A. Asli-Ardeh
Sensitivity analysis of a parabolic trough concentrator with linear V-shape cavity
Energy Sci. Eng., 8 (2020), pp. 3544-3560
View at publisher ↗ Crossref ↗ View in Scopus ↗ Google Scholar ↗

[8] K. Reddy, S.K. Natarajan, G. Veershetty
Experimental performance investigation of modified cavity receiver with fuzzy focal solar dish concentrator
Renew. Energy, 74 (2015), pp. 148-157
View PDF View article View in Scopus ↗ Google Scholar ↗

[9] K.H. Kumar, A. Rajan, M. Karmakar, B. Mondal, P.K. Mallisetty, K. Reddy
Comparative thermal assessment of Al2O3/EG and ZnO/EG as heat transfer fluids in solar parabolic dish receiver
Renew. Energy, 249 (2025), Article 123216
View PDF View article View in Scopus ↗ Google Scholar ↗

[10] R. Loni, A. Kasaeian, O. Mahian, A.Z. Sahin, S. Wongwises
Exergy analysis of a solar organic rankine cycle with square prismatic cavity receiver

Int. J. Exergy, 22 (2017), p. 103

View at publisher ↗ Crossref ↗ View in Scopus ↗ Google Scholar ↗

[11] M.H. Farhat, Y. Mazloum, S. Wakim, W.B. Nader, M. ALEbrahim, N. Ghareeb
Energy optimization of parabolic dish solar concentrator coupled to organic rankine cycle: experimental and analytical investigation of cavity receiver design and covering effects
Int. J. Thermofluids, 23 (2024), Article 100730

View PDF View article View in Scopus ↗ Google Scholar ↗

[12] R. Loni, E.A. Asli-Areh, B. Ghobadian, A. Kasaeian, S. Gorjian, G. Najafi, E. Bellos
Research and review study of solar dish concentrators with different nanofluids and different shapes of cavity receiver: experimental tests
Renew. Energy, 145 (2020), pp. 783-804

View PDF View article View in Scopus ↗ Google Scholar ↗

[13] T. Venkatachalam, M. Cheralathan
Effect of aspect ratio on thermal performance of cavity receiver for solar parabolic dish concentrator: an experimental study
Renew. Energy, 139 (2019), pp. 573-581

View PDF View article View in Scopus ↗ Google Scholar ↗

[14] A. Rafiei, A.S. Alsagri, S. Mahadzir, R. Loni, G. Najafi, A. Kasaeian
Thermal analysis of a hybrid solar desalination system using various shapes of cavity receiver: cubical, cylindrical, and hemispherical
Energy Convers. Manage., 198 (2019), Article 111861

View PDF View article View in Scopus ↗ Google Scholar ↗

[15] R. Loni, E.A. Asli-Ardeh, B. Ghobadian, A. Kasaeian, E. Bellos
Energy and exergy investigation of alumina/oil and silica/oil nanofluids in hemispherical cavity receiver: experimental study

Energy, 164 (2018), pp. 275-287

View PDF View article View in Scopus ↗ Google Scholar ↗

[16] A. Kasaeian, A. Kouravand, M.A.V. Rad, S. Maniee, F. Pourfayaz
Cavity receivers in solar dish collectors: a geometric overview
Renew. Energy, 169 (2021), pp. 53-79

View PDF View article View in Scopus ↗ Google Scholar ↗

[17] A.A. Abed, M.R. El-Marghany, W.M. El-Awady, A.M. Hamed
Recent advances in parabolic dish solar concentrators: receiver design, heat loss reduction, and nanofluid optimization for enhanced efficiency and applications
Solar Energy Mater. Solar Cells, 273 (2024), Article 112930

View PDF View article View in Scopus ↗ Google Scholar ↗

[18] S. Pavlovic, A.M. Daabo, E. Bellos, V. Stefanovic, S. Mahmoud, R.K. Al-Dadah
Experimental and numerical investigation on the optical and thermal performance of solar parabolic dish and corrugated spiral cavity receiver
J. Clean. Prod., 150 (2017), pp. 75-92

View PDF View article View in Scopus ↗ Google Scholar ↗

[19] R. Loni, E.A. Asli-Ardeh, B. Ghobadian, M. Ahmadi, E. Bellos
GMDH modeling and experimental investigation of thermal performance enhancement of hemispherical cavity receiver using MWCNT/oil nanofluid
Solar Energy, 171 (2018), pp. 790-803

View PDF View article View in Scopus ↗ Google Scholar ↗

[20] W. Ye, W. Chaiyapa, Y. Li
A comparative study of energy governance on energy resilience: process tracing of China and Thailand's solar power development
Energy Strat. Rev., 55 (2024), Article 101500

View PDF View article View in Scopus ↗ Google Scholar ↗

[21] A. Eitan, S. Bukchin-Peles
Solar middle ground: nGOs as regulatory intermediaries in renewable energy governance
Earth Syst. Govern., 26 (2025), Article 100298
View PDF View article View in Scopus ↗ Google Scholar ↗

[22] A. Eitan
Negotiating the energy transition: governance trade-offs in solar deployment
Energy Strat. Rev., 61 (2025), Article 101854
View PDF View article View in Scopus ↗ Google Scholar ↗

[23] A.M. Maghfuri, R. Loni, S. Pavlovic, A. Kasaeian
Solar ORC system using vacuum cubical cavity receiver to improve energy governance
Therm. Sci. Eng. Prog., 60 (2025), Article 103388
View PDF View article View in Scopus ↗ Google Scholar ↗

[24] R. Loni, S. Pavlovic
Enhancing energy governance: 3E analyses of solar organic rankine cycles with vacuum spiral cavity receiver
Results Eng., 25 (2025), Article 104393
View PDF View article View in Scopus ↗ Google Scholar ↗

[25] R. Loni, S. Pavlovic
Innovating energy governance: the role of nanofluid-enhanced solar vacuum hemispherical cavity receivers
Sustainable Energy Technol. Assess., 75 (2025), Article 104255
View PDF View article View in Scopus ↗ Google Scholar ↗

[26] M.M.N. Joybari, S. Rezaei, R. Loni, S.M.P. Zat

Pioneering solutions in renewable energy governance for reducing energy imbalance: a systematic review of global practices and implications for Iran
Energy Convers. Manage. X (2025), Article 101456
Google Scholar ↗

[27] A. Refiei, R. Loni, G. Najafi, A. Sahin, E. Bellos
Effect of use of MWCNT/oil nanofluid on the performance of solar organic Rankine cycle
Energy Rep., 6 (2020), pp. 782-794
View PDF View article View in Scopus ↗ Google Scholar ↗

[28] M. Gunther, R. Shahbazfar, Solar dish technology, Advanced CSP teaching materials, (2011) 1–63.
Google Scholar ↗

[29] R. Loni, E.A. Asli-Ardeh, B. Ghobadian, A. Kasaeian, S. Gorjian
Numerical and experimental investigation of wind effect on a hemispherical cavity receiver
Appl. Therm. Eng., 126 (2017), pp. 179-193
View PDF View article View in Scopus ↗ Google Scholar ↗

[30] E.A. Loni, B. Ghobadian, A. Kasaeian
Experimental study of carbon nano tube/oil nanofluid in dish concentrator using a cylindrical cavity receiver: outdoor tests
Energy Convers. Manage., 165 (2018), pp. 593-601
View in Scopus ↗ Google Scholar ↗

[31] R. Loni, A. Kasaeian, E.A. Asli-Ardeh, B. Ghobadian, S. Gorjian
Experimental and numerical study on dish concentrator with cubical and cylindrical cavity receivers using thermal oil
Energy, 154 (2018), pp. 168-181
View PDF View article View in Scopus ↗ Google Scholar ↗

[32] R. Loni, E.A. Asli-Ardeh, B. Ghobadian, A. Kasaeian, E. Bellos
Thermal performance comparison between Al2O3/oil and SiO2/oil nanofluids in cylindrical cavity receiver based on experimental study
Renew Energy, 129 (2018), pp. 652-665
View PDF View article View in Scopus ↗ Google Scholar ↗

[33] R. Loni, E.A. Asli-Ardeh, B. Ghobadian, A. Kasaeian
Experimental study of carbon nano tube/oil nanofluid in dish concentrator using a cylindrical cavity receiver: outdoor tests
Energy Convers. Manage., 165 (2018), pp. 593-601
View PDF View article View in Scopus ↗ Google Scholar ↗

[34] A.H. Arkian, G. Najafi, S. Gorjian, R. Loni, E. Bellos, T. Yusaf
Performance assessment of a solar dryer system using small parabolic dish and alumina/oil nanofluid: simulation and experimental study
Energies, 12 (2019), p. 4747
Crossref ↗ View in Scopus ↗ Google Scholar ↗

[35] J.R. Taylor
An Introduction to Error analysis: the Study of Uncertainties in Physical Measurements
MIT Press (2022)
Google Scholar ↗

[36] S. Ayele, W. Shen, Y. Mulugetta, T.K. Worako
Governance of renewable energy procurement via private suppliers: the Ethiopian experience
Energy Policy, 184 (2024), Article 113889
View PDF View article View in Scopus ↗ Google Scholar ↗

Cited by (0)